

Gravitational bending angle of light with finite-distance corrections in stationary axisymmetric spacetimes

Toshiaki Ono

February 21, 2019

Abstract

The bending angle of light in a static, spherically symmetric and asymptotically flat spacetime has been recently discussed by using the Gauss-Bonnet theorem in differential geometry, especially by taking account of the finite distance from a lens object to a light source and a receiver [Ishihara, Suzuki, Ono, Asada, Phys. Rev. D **95**, 044017 (2017)]. In this thesis, we investigate a possible extension of the method of calculating the bending angle of light to stationary, axisymmetric and asymptotically flat spacetimes. For this purpose, we consider the light rays on the equatorial plane in a stationary, axisymmetric and asymptotically flat spacetime. We introduce a spatial metric (we call this metric a generalized optical metric) to define the bending angle of light in the finite-distance situation. We show that the proposed bending angle of light is coordinate-invariant by using the Gauss-Bonnet theorem. The non-vanishing geodesic curvature of the photon orbit with the generalized optical metric is caused in gravitomagnetism, even though the light ray in the four-dimensional spacetime follows a null geodesic. However, the geodesic curvature of the photon orbit with the optical metric in a static, spherically symmetric and asymptotically flat spacetime becomes zero. Finally, we apply the proposed approach of calculating the bending angle of light to the Kerr spacetime and the rotating Teo wormhole as examples in order to demonstrate how the bending angle of light is computed by the present method. According to the result of Kerr case, the finite-distance correction to the gravitomagnetic bending angle of light due to the Sun's spin is around a pico-arcsecond level where we assume that an receiver at the Earth sees the light bending by the solar mass. In addition, the finite-distance corrections for Sgr A* also is estimated to be small (a nano-arcsecond level). Therefore,

the gravitomagnetic finite-distance corrections for these objects are improbable to be observed with present technology. Our results can recover the results of the previous works, if we take the infinite-distance limit.

Acknowledgment

I would like to express my sincere gratitude to Prof. Hideki Asada whose enormous support and perceptive comments were invaluable during the course of my study. I also owe a very important debt to Kei Yamada, Ashahi Ishihara and Yuuiti Sendouda whose opinions and information have helped me very much throughout the production of this study. I am also thankful to all members of our group at Hirosaki University. I would also like to express my gratitude to my family for their support and warm encouragements. Finally, I thank all who have supported me.

Contents

1	Introduction	4
1.1	Motivation	5
2	Bending angle of light axially symmetric and stationary space-times	9
2.1	The Gauss-Bonnet theorem	9
2.2	Stationary, axisymmetric spacetime and the optical metric . .	11
2.3	The Gaussian curvature on the equatorial plane	15
2.4	Geodesic curvature on the equatorial plane	16
2.4.1	The tangent vector and the acceleration vector of a photon orbit for the generalized optical metric	16
2.4.2	Geodesic curvature of a photon orbit	19
2.4.3	Geodesic curvature of a circular arc segment with an infinite radius	21
2.5	Impact parameter and the future directions of light ray at the receiver and source	22
2.6	Bending angle of light	26
3	Application to the Kerr spacetime	29
3.1	Kerr spacetime and γ_{ij}	29
3.2	The Gaussian curvature on the equatorial plane	33

3.3	Path integral of κ_g of photon orbit	35
3.4	ϕ_{RS} part	36
3.5	Ψ parts	37
3.6	Bending angle of light in Kerr spacetime	38
3.7	Finite-distance corrections to the gravitomagnetic bending angle of light	41
3.8	Possible astronomical applications	42
4	Application to rotating Teo wormhole	48
4.1	Rotating Teo wormhole and optical metric	48
4.2	Gaussian curvature	50
4.3	Geodesic curvature of photon orbit	51
4.4	ϕ_{RS} part	52
4.5	Ψ parts	53
4.6	Bending angle of light	53
4.7	Finite-distance corrections to the bending angle of light	55
5	Conclusion	58
A	Detailed calculations of the bending angle by a Kerr black hole at $O(M^2/b^2)$ and $O(a^2/b^2)$	60
B	Relation to the lens equation, the magnitude etc.	65

Chapter 1

Introduction

Gravitational red shift, Mercury's orbital(apsidal) precession, gravitational time delay of light and deflection of light are particularly well-known experiments in order to verify general relativity in the solar system [1–6].

The gravitational bending of light by mass led to the first experimental confirmations of the theory of general relativity [7] in 1919 [8]. In cosmology and modern astronomy, gravitational lensing is widely used as one of the important tools for probing dark energy, dark matter and extrasolar planets. The deflection of light is also of theoretical importance, especially for studying a null structure of a spacetime. A lot of calculations of the gravitational bending of light have been done not only for black holes [9–21] but also for other objects such as wormholes and gravitational monopoles [22–34]. For example, the analytical solution for light trajectories in the Schwarzschild spacetime was investigated by Hagihara [9], where the expressions involve incomplete elliptic integrals of the first kind; strong gravitational lensing in a Schwarzschild black hole was considered by Frittelli, Kling and Newman [15] and by Virbhadra and Ellis [16]. More comprehensive investigation was conducted by Virbhadra [17]; Virbhadra, Narasimha and Chitre [18] studied distinctive lensing features of naked singularities; Virbhadra and Ellis [19] and

Virbhadra and Keeton [20] later investigated strong gravitational lensing by naked singularities; lensing by naked singularities to test the cosmic censorship hypothesis was discussed by DeAndrea and Alexander [27]; Reissner-Nordström black hole lensing was studied by Eiroa, Romero and Torres [22]; Perlick [28] investigated the lensing by a Barriola-Vilenkin monopole and also that by an Ellis wormhole; Kitamura, Nakajima and Asada proposed a lens model whose gravitational potential declines as $1/r^n$ [29] in order to study the gravitational lensing by exotic matter (or energy) [30–33] that might follow a non-standard equation of state. See Tsukamoto et. al. [34] for its possible connection to the Tangherlini solution to the higher-dimensional Einstein equation.

In next section, we describe a motivation for studying a finite-distance correction to the bending angle of light with paying attentions to particularly important previous works by Gibbons and Werner (2008) [35] and Werner (2012) [36].

1.1 Motivation

Under the assumptions that

- The source is a point source,
- The source and the receiver are located at infinity from a lens object,
- The distribution of mass is spherically symmetric in an asymptotically flat spacetime (the lens object is a Schwarzschild black hole),

the bending angle of light α is

$$\alpha = \frac{4GM}{c^2 b} + \mathcal{O}\left(\frac{M^2}{b^2}\right) = \frac{2r_g}{b} + \mathcal{O}\left(\frac{r_g^2}{b^2}\right), \quad (1.1)$$

where G is the gravitational constant, M is the mass of the lens object, b is the impact parameter of photon, c is the velocity of light, $r_g = \frac{2GM}{c^2}$ is Schwarzschild radius and we used the weak field approximation ($\frac{M}{b} \ll 1$). This shows that the leading term of the bending angle of light is comparable to the linear post-Newtonian effect.

Gibbons and Werner proposed an alternative way of deriving the deflection angle of light [35]. They considered two different domains: one (Figure 1.1, D_1) bounded by two light rays, to exhibit the connection between topology and multiple paths; and the other (Figure 1.1, D_2) bounded by one light ray and a non-geodesic circular arc, to compute the asymptotic bending angle. They suggested that the asymptotic bending angle of light can be written as a surface integral of the Gaussian curvature over the domain D_2 . They performed the surface integration only for the asymptotic case, for which they assumed the observer and source are in the asymptotically Euclidean region. Namely, the angles at the location of the observer and source are defined only in Euclidean space. Ishihara et al. have recently extended Gibbons and Werner's method in order to investigate finite-distance corrections in the weak deflection case (corresponding to a large impact parameter case) [37] and also in the strong deflection limit for which the photon orbits may have a winding number larger than unity [38]. In particular, the asymptotic receiver and source have not been assumed.

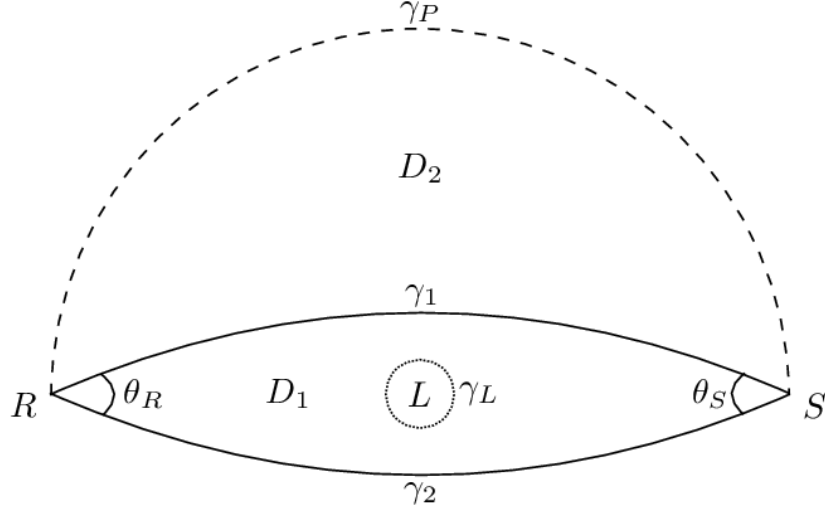


Figure 1.1: Schematic figure for the Gibbons and Werner approach. Two geodesics γ_1 and γ_2 from the source S to the receiver R are deflected by a lens L . The geodesic γ_L is corresponding to the photon sphere. γ_P is a circular arc with an infinite radius. D_1 is a domain with boundary curves γ_1 , γ_2 and γ_L . D_2 is a domain with boundary curves γ_1 and γ_P .

Werner [36] later proposed an extension of Gibbons and Werner's method to Kerr spacetime by using the Kerr-Randers optical geometry. To be more precise, he used the osculating Riemann approach in Finsler geometry in order to discuss the lensing by a Kerr black hole, for which the metric can be written in the Randers form. However, this approach requires that the endpoints (namely, the source and the receiver) of the photon orbit are in the Euclidean space, for which angles can be defined in a straightforward

manner.

This requirement is mainly because jump angles at the vertices in the Gauss-Bonnet theorem are problematic in formulating Finsler geometry. In other words, in the optical geometry it is possible to define the external angle of the vertex as the inner product of two vectors. In Finsler geometry, however, the external angle of the vertex cannot be defined by inner product because the metric depends on the coordinates and the vectors. Namely, it is unlikely that the Finsler geometry can be conveniently used for computing the finite-distance corrections.

In actual fact, a star or galaxy as a lens object has a spin angular momentum. In addition, the distances from lens to the source and the receiver are not infinity. The main purpose of this thesis is to investigate a possible extension of calculations [37] of the bending angle of light in a stationary, axisymmetric and asymptotically flat spacetime, particularly in order to find finite-distance corrections.

For this purpose, we investigate the deflection of light in stationary, axisymmetric and asymptotically flat spacetimes, especially by taking account of the finite distance from a lens object to a light source and a receiver in Chapter 2. In Chapter 3, we discuss how to compute the gravitational deflection angle of light by the proposed method, by using the Kerr metric as a known example of the stationary and axisymmetric spacetimes. In Chapter 4, we shall apply the proposed approach to a rotating Teo wormhole. Chapter 5 is devoted to the conclusion. In Appendix B, we discuss the relation between the lens equation, shear of image, magnification and the bending angle of light with finite-distance correction.

Throughout this thesis, we use the unit of $G = c = 1$. In the following, ϕ_R and ϕ_S denote the longitudes of the receiver and the source, respectively. r_R and r_S denote the radial coordinate distances from the lens object to the receiver and the source, respectively.

Chapter 2

Bending angle of light axially symmetric and stationary spacetimes

In this chapter, we discuss a possible extension of the method of calculating the bending angle of light to stationary and axisymmetric spacetimes. In particular, it is shown that the proposed definition of the bending angle is coordinate-invariant by using the Gauss-Bonnet theorem. We provide a brief explanation of the Gauss-Bonnet theorem in differential geometry.

2.1 The Gauss-Bonnet theorem

The Gauss-Bonnet theorem: Suppose that T is a two-dimensional orientable surface with boundaries ∂T_a ($a = 1, 2, \dots, N$) that are differentiable curves. (See Figure 2.1.) Let the jump angles between the curves be θ_a ($a =$

$1, 2, \dots, N$). Then, the Gauss-Bonnet theorem can be expressed as [39]

$$\iint_T K dS + \sum_{a=1}^N \int_{\partial T_a} \kappa_g d\ell + \sum_{a=1}^N \theta_a = 2\pi, \quad (2.1)$$

where K denotes the Gaussian curvature of the surface T , dS is the area element of the surface, κ_g means the geodesic curvature of ∂T_a , and ℓ is the line element along the boundary. The sign of the line element is chosen such that it is compatible with the orientation of the surface.

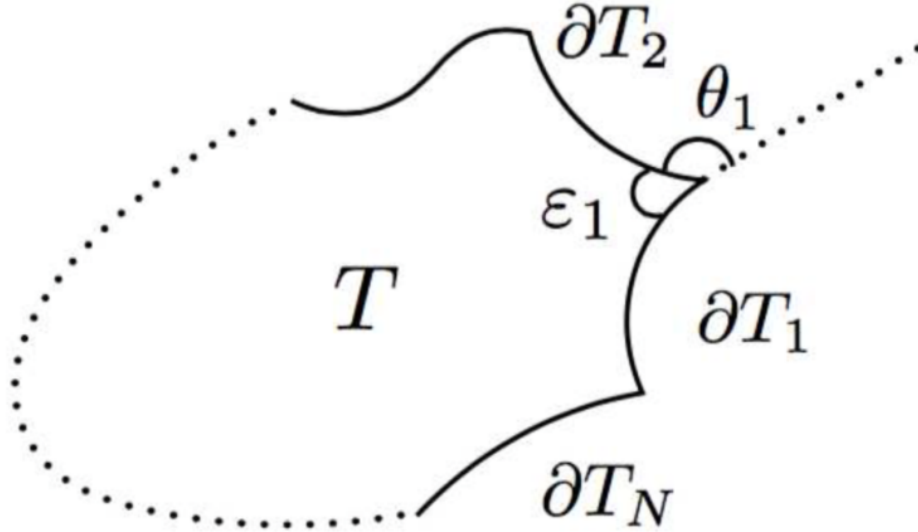


Figure 2.1: Schematic figure for the Gauss-Bonnet theorem. T is the closed surface. The boundaries of T are denoted by ∂T_i ($i = 1, \dots, N$). θ_i ($i = 1, \dots, N$) is the jump angle at vertices

2.2 Stationary, axisymmetric spacetime and the optical metric

Henceforth, we assume a stationary and axisymmetric spacetime, for which we shall define the gravitational bending angle of light by using the Gauss-Bonnet theorem. First, let us consider a stationary axisymmetric spacetime. The line element for this spacetime is [40–42]

$$\begin{aligned} ds^2 &= g_{\mu\nu} dx^\mu dx^\nu \\ &= -A(y^p, y^q) dt^2 - 2H(y^p, y^q) dt d\phi \\ &\quad + F(y^p, y^q) \gamma_{pq} dy^p dy^q + D(y^p, y^q) d\phi^2, \end{aligned} \quad (2.2)$$

where μ, ν run from 0 to 3, p, q take 1 and 2, t and ϕ coordinates are associated with the Killing vectors, and γ_{pq} is a two-dimensional symmetric tensor. It is more convenient to reexpress this metric into a form in which γ_{pq} is diagonalized. The present thesis prefers the polar coordinates rather than the cylindrical ones, because the Kerr metric and the rotating Teo wormhole metric in the polar coordinates are considered in Section 3 and Section 4 respectively. In the polar coordinates, Eq. (2.2) is rewritten as [43]

$$\begin{aligned} ds^2 &= -A(r, \theta) dt^2 - 2H(r, \theta) dt d\phi \\ &\quad + B(r, \theta) dr^2 + C(r, \theta) d\theta^2 + D(r, \theta) d\phi^2, \end{aligned} \quad (2.3)$$

where we assume a local reflection symmetry with respect to the equatorial plane $\theta = \frac{\pi}{2}$ as

$$\left. \frac{\partial g_{\mu\nu}}{\partial \theta} \right|_{\theta=\frac{\pi}{2}} = 0. \quad (2.4)$$

The functions are $A(r, \theta) > 0, B(r, \theta) > 0, C(r, \theta) > 0, D(r, \theta) > 0$ and $H(r, \theta) > 0$.

This assumption is needed for the existence of a photon orbit on the equatorial plane.

The null condition $ds^2 = 0$ is solved for dt as [44]

$$dt = \sqrt{\gamma_{ij} dx^i dx^j} + \beta_i dx^i, \quad (2.5)$$

where i, j run from 1 to 3, γ_{ij} and β_i are defined as

$$\gamma_{ij} dx^i dx^j \equiv \frac{B(r, \theta)}{A(r, \theta)} dr^2 + \frac{C(r, \theta)}{A(r, \theta)} d\theta^2 + \frac{A(r, \theta)D(r, \theta) + H^2(r, \theta)}{A^2(r, \theta)} d\phi^2, \quad (2.6)$$

$$\beta_i dx^i \equiv - \frac{H(r, \theta)}{A(r, \theta)} d\phi. \quad (2.7)$$

This spatial metric $\gamma_{ij} (\neq g_{ij})$ may define the arc length (ℓ) along the photon orbit as

$$d\ell^2 \equiv \gamma_{ij} dx^i dx^j, \quad (2.8)$$

for which γ^{ij} is defined by $\gamma^{ij}\gamma_{jk} = \delta^i_k$. Note that ℓ defined in this way is an affine parameter along the light ray. See e.g. Appendix of Ref. [44] for the proof on the affine parameter. γ_{ij} defines a 3-dimensional Riemannian space $^{(3)}M$ where the photon orbit is described as a spatial curve. If we consider the bending angle of light in a static, spherically symmetric and asymptotically flat spacetime, however β_i is zero and γ_{ij} is the optical metric as is well known. The photon orbit is described as a geodesic in a 3-dimensional Riemannian space. In this section and after, we call γ_{ij} the generalized optical metric.

Let us apply the Gauss-bonnet theorem to such a closed surface (figure

2.2), the Gauss-Bonnet theorem becomes

$$\iint_{R_\infty \square_S^{S_\infty}} K dS + \int_R^S \kappa_g d\ell + \int_{S_\infty}^{R_\infty} \bar{\kappa}_g d\ell + [\Psi_R + (\pi - \Psi_S) + \pi] = 2\pi, \quad (2.9)$$

where S and R mean the source and the receiver and the subscript ∞ shows an asymptotic point. We note that the geodesic curvatures of the path from S to S_∞ and the path from R to R_∞ are both 0 since these paths are geodesic. κ_g is the geodesic curvature of the photon orbit and $\bar{\kappa}_g$ is the geodesic curvature of the circular arc segment of an infinite radius.

In Section 2.3, we consider the Gaussian curvature on the equatorial plane. In Section 2.4, we discuss the geodesic curvature on the equatorial plane. In Section 2.5, we investigate the jump angles at the source and the receiver. In order to calculate the geodesic curvature and the jump angles at the source and the receiver, we study the tangent vector and the acceleration vector of the photon orbit in Section 2.4.1.

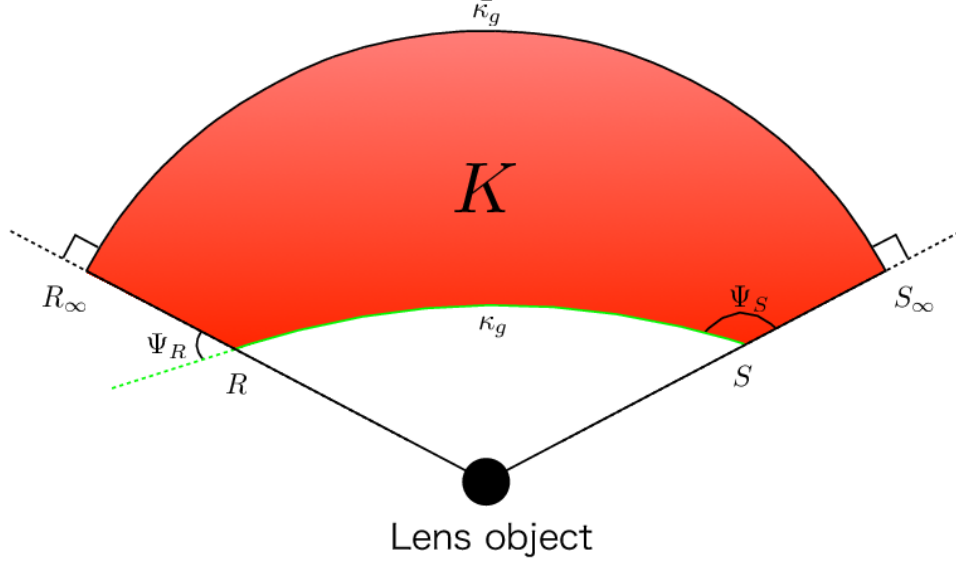


Figure 2.2: Quadrilateral ${}^R_{R_\infty}\square^S_{S_\infty}$ on the equatorial plane is embedded in 3-dimensional space associated with the generalized optical metric γ_{ij} . The point S means the position of the source. The point R means the position of the receiver. The Gaussian curvature K is of the red region. The green curve is a light ray in the space associated with γ_{ij} . Its geodesic curvature is denoted by κ_g . The geodesic curvature $\bar{\kappa}_g$ is of the circular arc segment with radius $R_\infty = S_\infty$.

2.3 The Gaussian curvature on the equatorial plane

The Gaussian curvature on the equatorial plane is expressed by the 2-dimensional Riemann tensor ${}^{(2)}R_{r\phi r\phi}$ as [36]

$$K = \frac{{}^{(2)}R_{r\phi r\phi}}{\det \gamma_{ij}^{(2)}} = \frac{1}{\sqrt{\det \gamma_{ij}^{(2)}}} \left[\frac{\partial}{\partial \phi} \left(\frac{\sqrt{\det \gamma_{ij}^{(2)}}}{\gamma_{rr}^{(2)}} {}^{(2)}\Gamma_{rr}^{\phi} \right) - \frac{\partial}{\partial r} \left(\frac{\sqrt{\det \gamma_{ij}^{(2)}}}{\gamma_{rr}^{(2)}} {}^{(2)}\Gamma_{r\phi}^{\phi} \right) \right], \quad (2.10)$$

where ${}^{(2)}R_{r\phi r\phi}$ and ${}^{(2)}\Gamma_{jk}^i$ are associated with the generalized optical metric γ_{ij} of the equatorial plane. $\det \gamma_{ij}^{(2)}$ is the determinant of the generalized optical metric of the equatorial plane.

In the polar coordinates, dS in Eq.(2.9) becomes

$$dS = \sqrt{\det \gamma^{(2)}} dr d\phi. \quad (2.11)$$

Therefore, the surface integral of the Gaussian curvature in Eq.(2.9) is rewritten as

$$\iint_{\int_R^{\infty} \square_S^{\infty}} K dS = \int_{\phi_S}^{\phi_R} \int_{r_{OE}}^{\infty} K \sqrt{\det \gamma^{(2)}} dr d\phi, \quad (2.12)$$

where r_{OE} is the solution of the orbit equation that can be obtained iteratively.

2.4 Geodesic curvature on the equatorial plane

Let us imagine a parameterized curve in a surface. The geodesic curvature of the parameterized curve means how different the curve is from the geodesic. The geodesic curvature of the parameterized curve is the surface-tangential component of acceleration (namely the geodesic curvature) of the curve, while the normal curvature is the surface-normal component of acceleration. The normal curvature has nothing to do with this thesis, because we consider the curve on the equatorial plane.

The geodesic curvature can be defined in the vector form as (see e.g. [47])

$$\kappa_g \equiv \mathbf{T}' \cdot (\mathbf{T} \times \mathbf{N}), \quad (2.13)$$

where we assume a parameterized curve with a parameter, \mathbf{T} is the unit tangent vector for the curve by reparameterizing the curve using its arc length, \mathbf{T}' is its derivative with respect to the parameter, and \mathbf{N} is the unit normal vector for the surface. It is a matter of course that the geodesic curvature of the curve becomes zero when the curve is the geodesic, because the acceleration vector \mathbf{T}' is zero.

2.4.1 The tangent vector and the acceleration vector of a photon orbit for the generalized optical metric

The unit tangent vector along the spatial curve is defined as

$$e^i \equiv \frac{dx^i}{d\ell}, \quad (2.14)$$

where ℓ is defined by Eq.(2.8).

Then, the arrival time T of a light from the source to the receiver is given

by the integral of Eq.(2.5),

$$T = \int_{t_S}^{t_R} dt = \int_S^R \left(\sqrt{\gamma_{ij} de^i de^j} + \beta_i de^i \right) d\ell, \quad (2.15)$$

where the subscripts S and R denote the source and the receiver, respectively. The light ray follows the Fermat's principle ($\delta T = 0$) [46]. Now, the Lagrangian is expressed as

$$\mathcal{L} = \sqrt{\gamma_{ij} e^i e^j} + \beta_i e^i. \quad (2.16)$$

We obtain

$$\frac{d}{d\ell} \frac{\partial \mathcal{L}}{\partial e^k} = \gamma_{ik} e^i{}_{,l} e^l + \gamma_{ik,l} e^i e^l + \beta_{k,i} e^i, \quad (2.17)$$

$$\frac{\partial \mathcal{L}}{\partial x^k} = \frac{1}{2} \gamma_{ij,k} e^i e^j + \beta_{i,k} e^i, \quad (2.18)$$

where we used $\gamma_{ij} e^i e^j = 1$ and the comma $(,)$ defines the partial derivative. Then, the Euler-Lagrange equation ($\frac{d}{d\ell} \frac{\partial \mathcal{L}}{\partial e^j} - \frac{\partial \mathcal{L}}{\partial x^j} = 0$) is calculated as

$$e^j{}_{,l} e^l + \gamma^{kj} \left(\gamma_{ik,l} e^i e^l - \frac{1}{2} \gamma_{il,k} e^i e^l \right) = \gamma^{kj} (\beta_{l,k} - \beta_{k,l}) e^l. \quad (2.19)$$

This gives the equation for the light ray as [44]

$$\frac{de^i}{d\ell} = -\gamma^{il} (\gamma_{lj,k} - \frac{1}{2} \gamma_{jk,l}) e^j e^k + \gamma^{ij} (\beta_{k,j} - \beta_{j,k}) e^k.$$

Therefore, the geodesic equation is

$$\begin{aligned}
e^i|_j e^j &= \frac{de^i}{d\ell} + {}^{(3)}\Gamma^i_{jk} e^j e^k \\
&= \frac{de^i}{d\ell} + \gamma^{il} (\gamma_{lj,k} - \frac{1}{2} \gamma_{jk,l}) e^j e^k \\
&= \gamma^{ij} (\beta_{k,j} - \beta_{j,k}) e^k,
\end{aligned} \tag{2.20}$$

where $|$ denotes the covariant derivative with respect to γ_{ij} . ${}^{(3)}\Gamma^i_{jk}$ denotes the Christoffel symbol associated with γ_{ij} .

The acceleration vector a^i is defined as

$$a^i \equiv e^i|_j e^j = \gamma^{ij} (\beta_{k|j} - \beta_{j|k}) e^k = \gamma^{ij} (\beta_{k,j} - \beta_{j,k}) e^k. \tag{2.21}$$

We can rewrite the cross product of \mathbf{A} and \mathbf{B} by using the Levi-Civita symbol ε_{ijk}

$$\sqrt{\gamma} \varepsilon_{ijk} A^j B^k = (\mathbf{A} \times \mathbf{B})_i. \tag{2.22}$$

Note that the Levi-Civita tensor ϵ_{ijk} in a three-dimensional satisfies space

$$\epsilon_{sjk} \epsilon^{slm} = \sqrt{\gamma} \varepsilon_{sjk} \frac{1}{\sqrt{\gamma}} \varepsilon^{slm} = \delta_j^l \delta_k^m - \delta_j^m \delta_k^l, \tag{2.23}$$

$$\epsilon_{sjk} \epsilon^s_{lm} = \gamma_{jl} \gamma_{km} - \gamma_{jm} \gamma_{kl}. \tag{2.24}$$

By using Eqs.(2.22),(2.23) and (2.24), we can rewrite Eq.(2.21) as

$$a^i = \gamma^{ij} e^k \epsilon_{sjk} (\nabla \times \boldsymbol{\beta})^s. \tag{2.25}$$

The vector a^i is the spatial vector that means the acceleration originated from β_i . In particular, a^i is caused in gravitomagnetism [45]. More precisely, this has an analogy to the acceleration by the Lorentz force $\propto \mathbf{v} \times (\nabla \times \mathbf{A}_m)$

in electromagnetism, where \mathbf{A}_m denotes the magnetic vector potential. The magnetic vector potential is a vector field, defined by $\mathbf{B} = \nabla \times \mathbf{A}_m$, $\mathbf{E} = -\nabla\phi - \frac{\partial\mathbf{A}_m}{\partial t}$, where \mathbf{B} and \mathbf{E} are the magnetic field and the electric field, respectively. ϕ is a electric potential (a scalar field).

We should note that γ_{ij} is not an induced metric. The photon orbit can deviate from a geodesic in $^{(3)}M$ with γ_{ij} if β_i does not vanish, even though the light ray in the four-dimensional spacetime obeys the null geodesic.

For a stationary and spherically symmetric spacetime, one can always find a set of suitable coordinates such that g_{0i} can vanish to lead to $a^i = 0$. In this case, the photon orbit becomes a spatial geodesic curve in $^{(3)}M$.

This thesis discusses an extension to axisymmetric cases, which allow $g_{0i} \neq 0$. Therefore, we have to take account of non-zero geodesic curvature κ_g along the photon orbit in the Gauss-Bonnet theorem. The geodesic curvature κ_g of a photon orbit is originated from the gravitomagnetic effect. This non-vanishing κ_g of the photon orbit makes a crucial difference from the previous papers [37, 38]

2.4.2 Geodesic curvature of a photon orbit

Eq. (2.13) can be rewritten in the tensor form as

$$\kappa_g = \epsilon_{ijk} N^i a^j e^k, \quad (2.26)$$

where \vec{T} and \vec{T}' correspond to e^k and a^j , respectively.

In this thesis, the acceleration vector of the photon orbit depends on β_i . Hence, the geodesic curvature of the photon orbit depends on β_i .

There can exist a non-vanishing integral of the geodesic curvature along the light ray in the Gauss-Bonnet theorem Eq. (2.1).

By substituting Eq. (2.21) into a^i in Eq. (2.26), we obtain

$$\begin{aligned}
\kappa_g &= \epsilon_{ijk} N^i \gamma^{jl} (\beta_{n|l} - \beta_{l|n}) e^n e^k \\
&= \gamma^{ja} N^i e^k e^b \epsilon_{ijk} \epsilon_{sab} (\nabla \times \beta)^s \\
&= \gamma^{ja} N^i e^k e^b \epsilon_{ijk} \epsilon_{sab} \epsilon^{sml} \beta_{l|m} \\
&= N^i e^k e^b \epsilon_i^a{}_{k} \epsilon_{sab} \epsilon^{sml} \beta_{l|m} \\
&= N_i e_k e^b \epsilon^{aik} \epsilon_{asb} \epsilon^{sml} \beta_{l|m} \\
&= N_i e_k e^b (\delta^i{}_s \delta^k{}_b - \delta^i{}_b \delta^k{}_s) \epsilon^{sml} \beta_{l|m} \\
&= -\epsilon^{ijk} N_i \beta_{j|k},
\end{aligned} \tag{2.27}$$

where we used $\gamma_{ij} e^i e^j = 1$ and $\gamma_{ij} e^i N^j = 0$. Then, the unit normal vector for the equatorial plane can be expressed as

$$N_p = \frac{1}{\sqrt{\gamma^{\theta\theta}}} \delta_p^\theta, \tag{2.28}$$

where we chose the upward direction without loss of generality.

For the equatorial case, one can show

$$\epsilon^{\theta pq} \beta_{q|p} = -\frac{1}{\sqrt{\gamma}} \beta_{\phi,r}, \tag{2.29}$$

where the comma denotes the partial derivative, we use $\epsilon^{\theta r\phi} = -1/\sqrt{\gamma}$ and we note $\beta_{r,\phi} = 0$ owing to the axisymmetry. By using Eqs. (2.28) and (2.29), an explicit form of κ_g in Eq. (2.27) is obtained as

$$\kappa_g = -\frac{1}{\sqrt{\gamma \gamma^{\theta\theta}}} \beta_{\phi,r}. \tag{2.30}$$

The line element for the path integral is obtained by using Eq.(2.8) as

$$d\ell = \sqrt{\gamma_{rr} \left(\frac{dr}{d\phi} \right)^2 + \gamma_{\phi\phi}} d\phi, \quad (2.31)$$

where we choose $\theta = \pi/2$.

2.4.3 Geodesic curvature of a circular arc segment with an infinite radius

We can obtain the geodesic curvature κ of the circular arc segment of radius R in flat space as

$$\kappa = \frac{1}{R}. \quad (2.32)$$

Then the geodesic curvature $\bar{\kappa}_g$ of a circular arc segment of radius $R_c = R_\infty = S_\infty$ is obtained as

$$\bar{\kappa}_g = \frac{1}{R_c}, \quad (2.33)$$

where the radius R_c is sufficiently larger than r_R and r_S , and the circular arc segment exists in the asymptotically flat region.

Eq.(2.8) becomes $d\ell^2 = dr^2 + r^2(d\theta^2 + \sin^2 \theta d\phi^2)$, because we assume that the spacetime is asymptotically flat. Then, the line element for the path integral of $\bar{\kappa}_g$ is obtained as

$$d\ell = R_c d\phi, \quad (2.34)$$

where we chose $\theta = \pi/2$ and $r = R_c$ because we focus on the line element of the circular arc segment .

Therefore, the path integral of $\bar{\kappa}_g$ in Eq.(2.9) can be rewritten as

$$\int_{S_\infty}^{R_\infty} \bar{\kappa}_g d\ell = \int_{\phi_S}^{\phi_R} d\phi = \phi_R - \phi_S = \phi_{RS}, \quad (2.35)$$

where we define the angular coordinate values of the receiver and the source as ϕ_R and ϕ_S , respectively.

2.5 Impact parameter and the future directions of light ray at the receiver and source

We study the orbit equation on the equatorial plane with Eq. (2.3). The Lagrangian in the equatorial plane is obtained as

$$\hat{\mathcal{L}} = -A(r)\dot{t}^2 - 2H(r)\dot{t}\dot{\phi} + B(r)\dot{r}^2 + D(r)\dot{\phi}^2, \quad (2.36)$$

where the dot denotes the derivative with respect to the affine parameter and the functions $A(r), B(r), D(r), H(r)$ mean, to be precise, $A(r, \pi/2), B(r, \pi/2), D(r, \pi/2), H(r, \pi/2)$ respectively.

The symmetry means the existence of conserved quantities along the geodesic. Now, the metric (or the Lagrangian $\hat{\mathcal{L}}$ in the 4-dimensional space-time) is independent of t and ϕ . Therefore,

$$\begin{aligned} \frac{d}{d\ell} \frac{\partial \hat{\mathcal{L}}}{\partial \dot{t}} &= 0, \\ \frac{d}{d\ell} \frac{\partial \hat{\mathcal{L}}}{\partial \dot{\phi}} &= 0. \end{aligned}$$

Then, associated with the two Killing vectors $\xi^\mu = (1, 0, 0, 0)$ and $\bar{\xi}^\mu =$

$(0, 0, 0, 1)$, respectively,

$$\begin{aligned}\frac{\partial \hat{\mathcal{L}}}{\partial \dot{t}} &= g_{\mu\nu} \xi^\mu k^\nu, \\ \frac{\partial \hat{\mathcal{L}}}{\partial \dot{\phi}} &= g_{\mu\nu} \bar{\xi}^\mu k^\nu,\end{aligned}\tag{2.37}$$

where $k^\mu = \frac{dx^\mu}{d\ell}$ is the tangent vector of the light ray in the 4-dimensional spacetime. There are two constants of motion

$$E = A(r)\dot{t} + H(r)\dot{\phi},\tag{2.38}$$

$$L = D(r)\dot{\phi} - H(r)\dot{t},\tag{2.39}$$

where E denotes energy of the photon and L means angular momentum of the photon. As usual, we define the impact parameter as

$$\begin{aligned}b &\equiv \frac{L}{E} \\ &= \frac{-H(r)\dot{t} + D(r)\dot{\phi}}{A(r)\dot{t} + H(r)\dot{\phi}} \\ &= \frac{-H(r) + D(r)\frac{d\phi}{dt}}{A(r) + H(r)\frac{d\phi}{dt}}.\end{aligned}\tag{2.40}$$

In terms of the impact parameter b , $\hat{\mathcal{L}} = 0$ leads to the orbit equation on the equatorial plane as

$$\left(\frac{dr}{d\phi}\right)^2 = \frac{A(r)D(r) + H^2(r)}{B(r)} \frac{D(r) - 2H(r)b - A(r)b^2}{[H(r) + A(r)b]^2},\tag{2.41}$$

where we used Eq.(2.3). Let us introduce $u \equiv 1/r$ to rewrite the orbit

equation as

$$\left(\frac{du}{d\phi}\right)^2 = F(u), \quad (2.42)$$

where $F(u)$ is

$$F(u) = \frac{u^4(AD + H^2)(D - 2Hb - Ab^2)}{B(H + Ab)^2}. \quad (2.43)$$

Finally, we examine the angles (Ψ_R, Ψ_S in figure 2.3) at the receiver and source positions. The unit tangent vector along the photon orbit in $^{(3)}M$ is e^i . On the equatorial plane, its components are obtained as

$$e^i = \frac{1}{\xi} \left(\frac{dr}{d\phi}, 0, 1 \right). \quad (2.44)$$

Here, ξ satisfies

$$\frac{1}{\xi} = \frac{A(r)[H(r) + A(r)b]}{A(r)D(r) + H^2(r)}, \quad (2.45)$$

which can be derived from $\gamma_{ij}e^ie^j = 1$ by using Eq. (2.41).

The unit radial vector in the equatorial plane is

$$R^i = \left(\frac{1}{\sqrt{\gamma_{rr}}}, 0, 0 \right), \quad (2.46)$$

where we choose the outgoing direction for a sign convention.

Therefore, by using the inner product between e^i and R^i , we can define the angle as

$$\begin{aligned} \cos \Psi &\equiv \gamma_{ij}e^iR^j \\ &= \sqrt{\gamma_{rr}} \frac{A(r)[H(r) + A(r)b]}{A(r)D(r) + H^2(r)} \frac{dr}{d\phi}, \end{aligned} \quad (2.47)$$

where Eqs. (2.44), (2.45) and (2.46) are used. This can be rewritten as

$$\sin \Psi = \frac{H(r) + A(r)b}{\sqrt{A(r)D(r) + H^2(r)}}, \quad (2.48)$$

where we use Eq. (2.41). Note that $\sin \Psi$ in Eq. (2.48) is more convenient in practical calculations, because it needs only local quantities, whereas $\cos \Psi$ by Eq. (2.47) needs the derivative as $dr/d\phi$. In addition, the range of this Ψ is $0 \leq \Psi \leq \pi$ and hence $\sin \Psi$ is always positive.

By substituting r_R and r_S into r of Eq.(2.48), we obtain $\sin \Psi_R$ and $\sin \Psi_S$, respectively. We can get Ψ_R and Ψ_S from inverse functions of $\sin \Psi_R$ and $\sin \Psi_S$. We note that the range of the principal value of $y = \arcsin x$ is $-\frac{\pi}{2} \leq y \leq \frac{\pi}{2}$ as usual. However, the range of Ψ_R (Ψ_S) is $0 \leq \Psi_R$ (Ψ_S) $\leq \pi$ so that by using the usual principal value, Eq.(2.48) for (Ψ_R) and (Ψ_S) become

$$\sin \Psi_R = \frac{H(r_R) + A(r_R)b}{\sqrt{A(r_R)D(r_R) + H^2(r_R)}}, \quad (2.49)$$

$$\sin(\pi - \Psi_S) = \frac{H(r_S) + A(r_S)b}{\sqrt{A(r_S)D(r_S) + H^2(r_S)}}, \quad (2.50)$$

respectively, because Ψ_R is an acute angle and Ψ_S is an obtuse angle from figure 2.3.

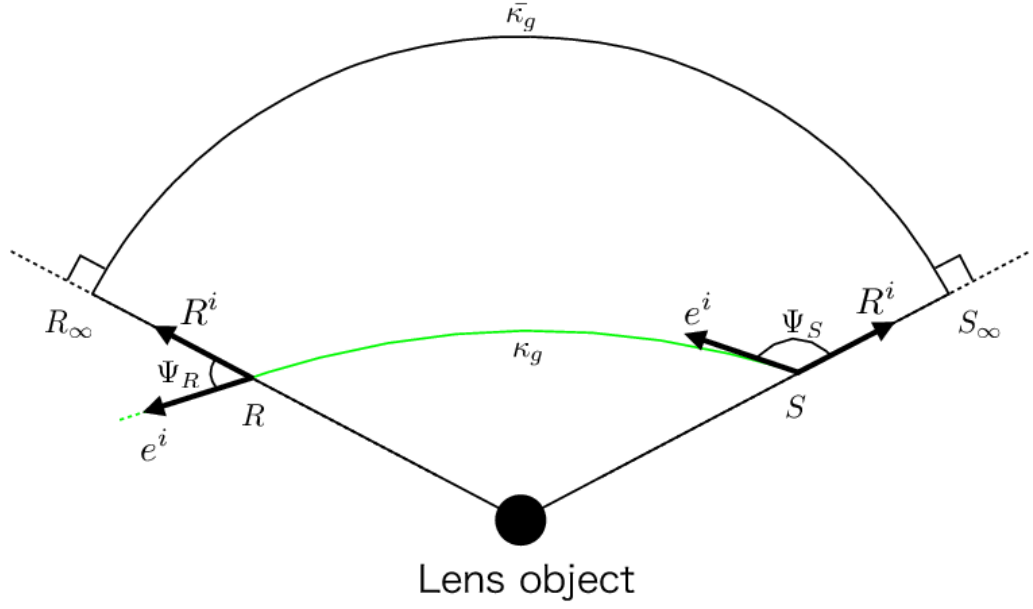


Figure 2.3: Ψ_R and Ψ_S . Ψ_R is obtained by using the inner product between the vector e^i and the vector R^i at the receiver point. Ψ_S is obtained by using the inner product between the vector e^i and the vector R^i at the source point.

2.6 Bending angle of light

For the equatorial case in the axisymmetric spacetime, we define

$$\alpha \equiv \Psi_R - \Psi_S + \phi_{RS}. \quad (2.51)$$

This definition seems to rely on a choice of the angular coordinate ϕ . By using the Gauss-Bonnet theorem Eq. (2.1), this is rewritten as

$$\alpha = - \iint_{\infty_R \square_S^\infty} K dS - \int_R^S \kappa_g d\ell, \quad (2.52)$$

where $d\ell$ is positive for the prograde motion of the photon and it is negative for the retrograde motion. Eq. (2.52) shows that α is three dimensional coordinate-invariant also for the axisymmetric case. Up to this point, equations for gravitational fields are not specified. Therefore, the above discussion and results are not limited within the theory of general relativity but they are applicable to a certain class of modified gravity theories only if the light ray in the four-dimensional spacetime obeys the null geodesic.

In order to find an interpretation of the definition of the bending angle of light in Eq.(2.51), we first consider a case of the thin lens approximation (see Figure 2.4). We apply the Gauss-Bonnet theorem to the quadrilateral in Figure 2.4 as

$$\begin{aligned} \alpha + (\pi - \Psi_R) + (\pi - \Psi_L) + \Psi_S &= 2\pi, \\ \alpha &= \Psi_R - \Psi_S + \Psi_L, \end{aligned} \quad (2.53)$$

where the Gaussian curvature of the quadrilateral is zero by calculating Eq.(2.10). The geodesic curvature of the sides of the quadrilateral is also zero, because these sides are geodesics. In Figure 2.2, we cannot define the angle Ψ_L , because the point of the lens is singular if the lens object is a black hole or an object including a singularity. What in Eq.(2.9) is related to Ψ_L of Eq.(2.53) ? It is $\int_{S_\infty}^{R_\infty} \bar{\kappa}_g d\ell = \phi_{RS}$. Therefore, we defined the bending angle of light as Eq.(2.51). We note that our definition of the bending angle is corresponding to an extension of the bending angle in the thin lens approximation, especially by taking account of the source and the receiver are in

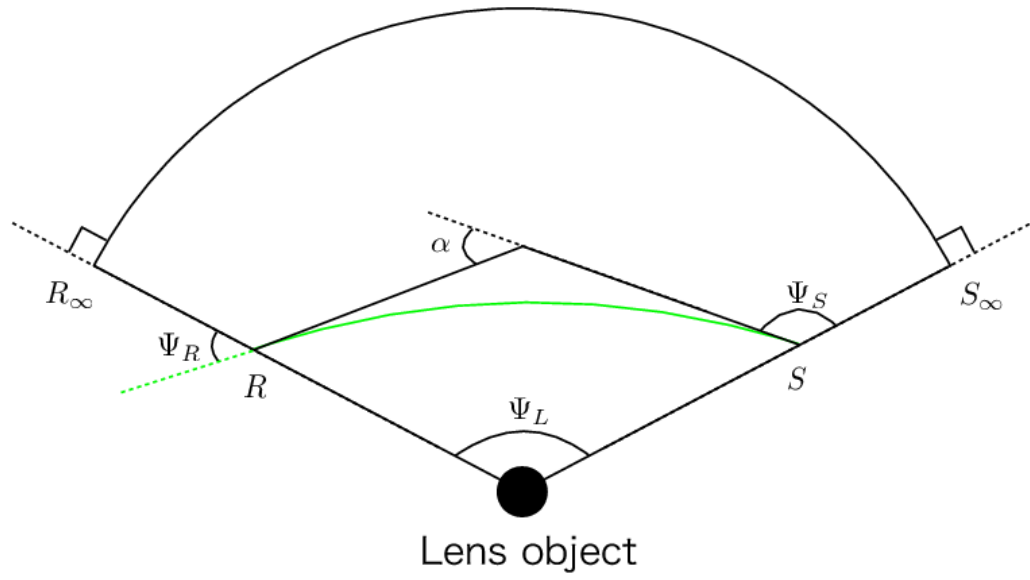


Figure 2.4: Thin lens approximation.

the curved space and the singularity at lens point.

Chapter 3

Application to the Kerr spacetime

3.1 Kerr spacetime and γ_{ij}

In this section, we focus on the bending angle of light in the Kerr spacetime as one of the most known examples with axisymmetry. The Kerr metric in the Boyer-Lindquist form is

$$ds^2 = - \left(1 - \frac{2Mr}{\Sigma} \right) dt^2 - \frac{4aMr \sin^2 \theta}{\Sigma} dt d\phi + \frac{\Sigma}{\Delta} dr^2 + \Sigma d\theta^2 + \left(r^2 + a^2 + \frac{2a^2 Mr \sin^2 \theta}{\Sigma} \right) \sin^2 \theta d\phi^2, \quad (3.1)$$

where Σ and Δ are defined as

$$\Sigma \equiv r^2 + a^2 \cos^2 \theta, \quad (3.2)$$

$$\Delta \equiv r^2 - 2Mr + a^2. \quad (3.3)$$

By using Eqs. (2.6) and (2.7), the generalized optical metric γ_{ij} and the

gravitomagnetic term β_i for the Kerr metric are given by

$$\gamma_{ij}dx^i dx^j = \frac{\Sigma^2}{\Delta(\Sigma - 2Mr)}dr^2 + \frac{\Sigma^2}{(\Sigma - 2Mr)}d\theta^2 + \left(r^2 + a^2 + \frac{2a^2Mr \sin^2 \theta}{(\Sigma - 2Mr)}\right) \frac{\Sigma \sin^2 \theta}{(\Sigma - 2Mr)}d\phi^2, \quad (3.4)$$

$$\beta_i dx^i = -\frac{2aMr \sin^2 \theta}{(\Sigma - 2Mr)}d\phi. \quad (3.5)$$

Note that γ_{ij} has no terms linear in the Kerr spin parameter a , because only g_{0i} in $g_{\mu\nu}$ has a linear term in a and $g_{0i} \propto H$ enters γ_{ij} through a quadratic form $g_{0i}g_{0j} \propto H^2$ as shown by Eq. (2.6).

For the present case, in order to calculate the Gaussian curvature K of the equatorial plane, the geodesic curvature κ_g of the light ray, the geodesic curvature $\bar{\kappa}_g$ of the circular arc of an infinite radius and the angles Ψ_R and Ψ_S , we employ the weak field and slow rotation approximations, for which M and a can be used as book-keeping parameters.

First, we obtain the orbit equation on the equatorial plane by using Eq.(2.41) as

$$\begin{aligned} \left(\frac{dr}{d\phi}\right)^2 &= \frac{b^2 \left\{ \frac{a^2}{b^2} + \frac{r}{b} \left(\frac{r}{b} - \frac{2M}{b} \right) \right\}^2 \left\{ \frac{a^2}{b^2} \left(\frac{2M}{b} + \frac{r}{b} \right) - \frac{4aM}{b^2} + \frac{2M}{b} - \frac{r}{b} + \frac{r^3}{b^3} \right\}}{\frac{r}{b} \left\{ \frac{2aM}{b^2} + \frac{r}{b} - \frac{2M}{b} \right\}^2} \\ &= \frac{r^4}{b^2} - r^2 + 2Mr - \frac{4r^3}{b^3}aM + \mathcal{O}(a^2), \end{aligned} \quad (3.6)$$

where we use the weak field and slow rotation approximations in the last line. There are no M squared terms in the last line. The orbit equation becomes

$$\left(\frac{du}{d\phi}\right)^2 = F(u) = \frac{1}{b^2} - u^2 + 2Mu^3 - \frac{4u}{b^3}aM + \mathcal{O}(a^2u^4). \quad (3.7)$$

Let us iteratively solve Eq.(3.7). In order to get the zero-th order solution,

we solve the reduced Eq.(3.7)

$$\left(\frac{du}{d\phi}\right)^2 = \frac{1}{b^2} - u^2 + \mathcal{O}(Mu^3, aMu^4, a^2u^4), \quad (3.8)$$

For this, the zero-th order solution is obtained as

$$u = \frac{\sin \phi}{b}, \quad (3.9)$$

where we use $\left.\frac{du}{d\phi}\right|_{\phi=\pi/2} = 0$ as the boundary condition. This condition shows that the closest approach of photon orbit is $r = r_0 = 1/u_0, \phi = \pi/2$. We assume that the linear-order solution with M is $u = \frac{\sin \phi}{b} + u_1(\phi)M$. In order to obtain $u_1(\phi)$, we substitute this solution into the Eq.(3.7) with terms linear in M

$$\left(\frac{du}{d\phi}\right)^2 = \frac{1}{b^2} - u^2 + 2Mu^3 + \mathcal{O}(aMu^4, a^2u^4), \quad (3.10)$$

then $u_1(\phi)$ is obtained as

$$u_1(\phi) = \frac{1}{b^2}(1 + \cos^2 \phi), \quad (3.11)$$

where we used the boundary condition mentioned above. The solution with a is in a form of $u = \frac{\sin \phi}{b} + \frac{M}{b^2}(1 + \cos^2 \phi) + u_2(\phi)a$. Since Eq.(3.7) does not include the terms linear in a , $u_2(\phi) = 0$. The solution with aM is $u = \frac{\sin \phi}{b} + \frac{M}{b^2}(1 + \cos^2 \phi) + u_3(\phi)aM$. We substitute this solution into Eq.(3.7)

$$\frac{aM}{b} \left\{ b^3 \frac{du_3(\phi)}{d\phi} \cos \phi + b^3 u_3(\phi) \sin \phi + 2 \sin \phi \right\} + \mathcal{O}(a^2u^4) = 0. \quad (3.12)$$

Hence, $u_3(\phi)$ is obtained as

$$u_3(\phi) = -\frac{2}{b^3}. \quad (3.13)$$

According to the above results, the iterative solution of Eq.(3.7) is obtained as

$$u = \frac{\sin \phi}{b} + \frac{M}{b^2}(1 + \cos^2 \phi) - \frac{2aM}{b^3} + \mathcal{O}\left(\frac{M^2}{b^3}, \frac{a^2}{b^3}\right). \quad (3.14)$$

Let us solve Eq.(3.14) for ϕ . We obtain ϕ as

$$\phi = \begin{cases} \arcsin(bu) + \frac{-2+b^2u^2}{b\sqrt{1-b^2u^2}}M + \frac{2aM}{b^2\sqrt{1-b^2u^2}} + \mathcal{O}\left(\frac{M^2}{b^3}, \frac{a^2}{b^3}\right) & (|\phi| < \frac{\pi}{2}) \\ \pi - \arcsin(bu) - \frac{-2+b^2u^2}{b\sqrt{1-b^2u^2}}M - \frac{2aM}{b^2\sqrt{1-b^2u^2}} + \mathcal{O}\left(\frac{M^2}{b^3}, \frac{a^2}{b^3}\right) & (\frac{\pi}{2} < |\phi|) \end{cases}, \quad (3.15)$$

where we can choose the range of ϕ to be $-\pi \leq \phi < \pi$ without loss of generality. In the following, the range of the angular coordinate value ϕ_S of the source point is $-\frac{\pi}{2} \leq \phi_S < \frac{\pi}{2}$ and the range of the angular coordinate value ϕ_R of the receiver point is $|\phi_R| > \frac{\pi}{2}$. We find $|bu| < 1$, because the square root in Eq.(3.15) must be real and nonzero, and the value of b and u are positive. Therefore, it ensures $0 < bu < 1$ in our calculation.

3.2 The Gaussian curvature on the equatorial plane

Let us calculate the Gaussian curvature by using Eq.(2.10). In the Kerr case, the Gaussian curvature is obtained as

$$\begin{aligned} K &= \frac{M(-6r(a^2 + M^2) + 6a^2M + 7Mr^2 - 2r^3)}{r^5(r - 2M)} \\ &= -\frac{2M}{r^3} + \mathcal{O}\left(\frac{M^2}{r^4}, \frac{a^2M}{r^5}\right), \end{aligned} \quad (3.16)$$

where we used the weak field and slow rotation approximations in the last line.

Next, we consider the area element on the equatorial plane by using Eq.(2.11). In the Kerr case, the area element of the equatorial plane becomes

$$dS = [r + 3M + \mathcal{O}(M^2/r)]drd\phi. \quad (3.17)$$

By using Eqs.(3.16) and (3.17), the surface integral of the Gaussian cur-

vature in Eq.(2.52) is obtained as

$$\begin{aligned}
- \iint_{R_\infty \square_S^{S_\infty}} K dS &= \int_{\phi_S}^{\phi_R} \int_{\infty}^{r_{OE}} \left(-\frac{2M}{r^3} r \right) dr d\phi + \mathcal{O} \left(\frac{M^2}{b^2}, \frac{aM^2}{b^3}, \frac{a^2M}{b^3} \right) \\
&= 2M \int_{\phi_S}^{\phi_R} \int_0^{\frac{1}{b} \sin \phi + \frac{M}{b^2} (1 + \cos^2 \phi) - \frac{2aM}{b^3}} du d\phi + \mathcal{O} \left(\frac{M^2}{b^2}, \frac{aM^2}{b^3}, \frac{a^2M}{b^3} \right) \\
&= 2M \int_{\phi_S}^{\phi_R} \left[u \right]_0^{\frac{1}{b} \sin \phi + \frac{M}{b^2} (1 + \cos^2 \phi) - \frac{2aM}{b^3}} d\phi + \mathcal{O} \left(\frac{M^2}{b^2}, \frac{aM^2}{b^3}, \frac{a^2M}{b^3} \right) \\
&= 2M \int_{\phi_S}^{\phi_R} \left[\frac{1}{b} \sin \phi \right] d\phi + \mathcal{O} \left(\frac{M^2}{b^2}, \frac{aM^2}{b^3}, \frac{a^2M}{b^3} \right) \\
&= \frac{2M}{b} \left[\cos \phi \right]_{\phi_R}^{\phi_S} + \mathcal{O} \left(\frac{M^2}{b^2}, \frac{aM^2}{b^3}, \frac{a^2M}{b^3} \right) \\
&= \frac{2M}{b} \left[\cos \phi_S - \cos \phi_R \right] + \mathcal{O} \left(\frac{M^2}{b^2}, \frac{aM^2}{b^3}, \frac{a^2M}{b^3} \right) \\
&= \frac{2M}{b} \left[\sqrt{1 - b^2 u_S^2} + \sqrt{1 - b^2 u_R^2} \right] + \mathcal{O} \left(\frac{M^2}{b^2}, \frac{aM^2}{b^3}, \frac{a^2M}{b^3} \right),
\end{aligned} \tag{3.18}$$

where r_{OE} in the first line is the solution of Eq.(3.6), we transform integration the variable as $r = 1/u$ in the second line, we used $\cos \phi_S = \sqrt{1 - b^2 u_S^2} + \mathcal{O}(M/b)$ and $\cos \phi_R = -\sqrt{1 - b^2 u_R^2} + \mathcal{O}(M/b)$ from Eq.(3.15) in the last line.

3.3 Path integral of κ_g of photon orbit

By substituting Eq. (3.5) into β_i in Eq. (2.30), we obtain

$$\begin{aligned}\kappa_g &= -\frac{2aM}{r^2(r-2M)} \left(\frac{1 - \frac{2M}{r} + \frac{a^2}{r^2}}{1 + \frac{a^2}{r^2} + \frac{2a^2M}{r^3}} \right)^{1/2} \\ &= -\frac{2aM}{r^3} + \mathcal{O}\left(\frac{aM^2}{r^4}\right),\end{aligned}\tag{3.19}$$

where we used the weak field and slow rotation approximations in the last line and the terms of $a^n M$ ($n \geq 2$) do not exist.

The line element for the path integral by Eq.(2.31) is obtained as

$$d\ell = \left[\frac{b}{\sin^2 \phi} + \mathcal{O}(M) \right] d\phi,\tag{3.20}$$

where we used Eq.(3.14) for a relation between r and ϕ .

By using Eqs.(3.20) and (3.19), the path integral of κ_g in Eq.(2.52) is computed as

$$\begin{aligned}-\int_R^S \kappa_g d\ell &= -\int_S^R \frac{2aM}{r^3} d\ell + \mathcal{O}\left(\frac{aM^2}{r^4}\right) \\ &= -\frac{2aM}{b^2} \int_{\phi_S}^{\phi_R} \sin \phi d\phi + \mathcal{O}\left(\frac{aM^2}{r^4}\right) \\ &= -\frac{2aM}{b^2} [\cos \phi_S - \cos \phi_R] + \mathcal{O}\left(\frac{aM^2}{b^3}\right) \\ &= -\frac{2aM}{b^2} [\sqrt{1-b^2 u_R^2} + \sqrt{1-b^2 u_S^2}] + \mathcal{O}\left(\frac{aM^2}{b^3}\right),\end{aligned}\tag{3.21}$$

where we assumed $d\ell > 0$ such that the orbital angular momentum of the photon can be aligned with the spin of the black hole and we use a linear

approximation of the photon orbit as $1/r = u = \sin \phi/b + \mathcal{O}(M/b^2, aM/b^3)$ from Eq.(3.14). Note that, in the retrograde case, the sign of $d\ell$ is negative and thus the magnitude of the above path integral remains the same but the sign of the integral is opposite.

3.4 ϕ_{RS} part

The displacement of the angular coordinate ϕ in Eq.(2.51) becomes

$$\begin{aligned}\phi_{RS} &= \int_S^R d\phi \\ &= 2 \int_0^{u_0} \frac{1}{\sqrt{F(u)}} du + \int_{u_S}^0 \frac{1}{\sqrt{F(u)}} du + \int_{u_R}^0 \frac{1}{\sqrt{F(u)}} du,\end{aligned}\quad (3.22)$$

where we used the orbit equation given by Eq.(2.42). By substituting Eq.(3.7) into $F(u)$ in Eq.(3.22), we obtain

$$\begin{aligned}\phi_{RS} &= \int_{u_S}^{u_0} \left(\frac{1}{\sqrt{u_0^2 - u^2}} + M \frac{u_0^3 - u^3}{(u_0^2 - u^2)^{3/2}} - 2aM \frac{u_0^3(u_0 - u)}{(u_0^2 - u^2)^{3/2}} \right) du \\ &\quad + \int_{u_R}^{u_0} \left(\frac{1}{\sqrt{u_0^2 - u^2}} + M \frac{u_0^3 - u^3}{(u_0^2 - u^2)^{3/2}} - 2aM \frac{u_0^3(u_0 - u)}{(u_0^2 - u^2)^{3/2}} \right) du \\ &\quad + \mathcal{O}(M^2 u_0^2, a^2 u_0^2) \\ &= \left(\frac{\pi}{2} - \arcsin \left(\frac{u_S}{u_0} \right) + M \frac{(2u_0 + u_S) \sqrt{u_0^2 - u_S^2}}{u_0 + u_S} - 2aM \frac{u_0^3 \sqrt{u_0^2 - u_S^2}}{u_0^2 + u_0 u_S} \right) \\ &\quad + \left(\frac{\pi}{2} - \arcsin \left(\frac{u_R}{u_0} \right) + M \frac{(2u_0 + u_R) \sqrt{u_0^2 - u_R^2}}{u_0 + u_R} - 2aM \frac{u_0^3 \sqrt{u_0^2 - u_R^2}}{u_0^2 + u_0 u_R} \right) \\ &\quad + \mathcal{O}(M^2 u_0^2, a^2 u_0^2),\end{aligned}\quad (3.23)$$

where we assumed the prograde case. For the retrograde case, the sign of the term linear in a becomes opposite. In Eq.(3.23), we rewrote the impact parameter b in terms of the closest approach u_0 in order to inte-

grate from u_S (or u_R) to u_0 . More precisely, Eq.(3.7) gives the relation between the impact parameter b and the inverse of the closest approach u_0 as $b = u_0^{-1} + M - 2aMu_0 + \mathcal{O}(M^2u_0, a^2u_0)$ in the weak field and slow rotation approximations. By using this relation, Eq. (3.23) can be rewritten in terms of b as

$$\begin{aligned} \phi_{RS} = & \pi - \arcsin(bu_S) - \arcsin(bu_R) + \frac{M(2 - b^2u_S^2)}{b\sqrt{1 - b^2u_S^2}} + \frac{M(2 - b^2u_R^2)}{b\sqrt{1 - b^2u_R^2}} \\ & - \frac{2aM}{b^2} \left[\frac{1}{\sqrt{1 - b^2u_S^2}} + \frac{1}{\sqrt{1 - b^2u_R^2}} \right] + \mathcal{O}(M^2/b^2, a^2/b^2). \end{aligned} \quad (3.24)$$

The first line recovers Eq. (32) of Ref. [37].

3.5 Ψ parts

For the Kerr metric Eq.(3.1), Eq.(2.49) becomes

$$\begin{aligned} \sin \Psi_R = & \frac{b}{r_R} \times \frac{1 - \frac{2M}{r_R} + \frac{2aM}{br_R}}{\sqrt{1 - \frac{2M}{r_R} + \frac{a^2}{r_R^2}}}, \\ = & \frac{b}{r_R} \left(1 - \frac{M}{r_R} + \frac{2aM}{br_R} \right) + \mathcal{O} \left(\frac{M^2}{r_R^2}, \frac{a^2}{r_R^2}, \frac{aM^2}{r_R^3} \right) \\ = & bu_R \left(1 - Mu_R + \frac{2aMu_R}{b} \right) + \mathcal{O}(M^2u_R^2, a^2u_R^2, aM^2u_R^3), \end{aligned} \quad (3.25)$$

and Eq.(2.50) is calculated as

$$\sin(\pi - \Psi_S) = bu_S \left(1 - Mu_S + \frac{2aMu_S}{b} \right) + \mathcal{O}(M^2u_S^2, a^2u_S^2, aM^2u_S^3), \quad (3.26)$$

where we used the weak field and slow rotation approximations and rewrote as $r_R = 1/u_R, r_S = 1/u_S$. We obtain Ψ_R and Ψ_S from Eqs.(3.25) and (3.26) as

$$\begin{aligned}
\Psi_R &= \arcsin \left[bu_R \left(1 - Mu_R + \frac{2aMu_R}{b} \right) \right] + \mathcal{O} (M^2u_R^2, a^2u_R^2, aM^2u_R^3) \\
&= \arcsin(bu_R) - \frac{Mbu_R^2}{\sqrt{1-b^2u_R^2}} + \frac{2aMu_R^2}{\sqrt{1-b^2u_R^2}} + \mathcal{O} (M^2u_R^2, a^2u_R^2, aM^2u_R^3), \\
\pi - \Psi_S &= \arcsin(bu_S) - \frac{Mbu_S^2}{\sqrt{1-b^2u_S^2}} + \frac{2aMu_S^2}{\sqrt{1-b^2u_S^2}} + \mathcal{O} (M^2u_S^2, a^2u_S^2, aM^2u_S^3).
\end{aligned} \tag{3.27}$$

By using these relations, we obtain the Ψ part in Eq.(2.51) as

$$\begin{aligned}
\Psi_R - \Psi_S &= \arcsin(bu_R) + \arcsin(bu_S) - \pi - \frac{Mbu_R^2}{\sqrt{1-b^2u_R^2}} - \frac{Mbu_S^2}{\sqrt{1-b^2u_S^2}} \\
&\quad + \frac{2aMu_R^2}{\sqrt{1-b^2u_R^2}} + \frac{2aMu_S^2}{\sqrt{1-b^2u_S^2}} + \mathcal{O} (M^2u_R^2, M^2u_S^2, a^2u_R^2, a^2u_S^2, aM^2u_R^3, aM^2u_S^3).
\end{aligned} \tag{3.28}$$

3.6 Bending angle of light in Kerr spacetime

The bending angle of light on the equatorial plane in the Kerr spacetime is expressed as Eq.(2.51) and Eq.(2.52). Let us confirm whether the two results coincide.

First, by substituting Eqs. (3.24) and (3.28) into Eq. (2.51), the deflection angle of light on the equatorial plane in the Kerr spacetime is obtained

as

$$\begin{aligned}
\alpha_{prog} &= \arcsin(bu_R) + \arcsin(bu_S) - \pi - \frac{Mbu_R^2}{\sqrt{1-b^2u_R^2}} - \frac{Mbu_S^2}{\sqrt{1-b^2u_S^2}} \\
&\quad + \frac{2aMu_R^2}{\sqrt{1-b^2u_R^2}} + \frac{2aMu_S^2}{\sqrt{1-b^2u_S^2}} \\
&\quad + \pi - \arcsin(bu_S) - \arcsin(bu_R) + \frac{M(2-b^2u_S^2)}{b\sqrt{1-b^2u_S^2}} + \frac{M(2-b^2u_R^2)}{b\sqrt{1-b^2u_R^2}} \\
&\quad - \frac{2aM}{b^2} \left[\frac{1}{\sqrt{1-b^2u_S^2}} + \frac{1}{\sqrt{1-b^2u_R^2}} \right] + \mathcal{O}\left(\frac{M^2}{b^2}\right) \\
&= \frac{2M}{b} \left(\sqrt{1-b^2u_R^2} + \sqrt{1-b^2u_S^2} \right) \\
&\quad - \frac{2aM}{b^2} \left(\sqrt{1-b^2u_R^2} + \sqrt{1-b^2u_S^2} \right) + \mathcal{O}\left(\frac{M^2}{b^2}\right), \tag{3.29}
\end{aligned}$$

where we assumed prograde motion of light. For the retrograde case, it is

$$\begin{aligned}
\alpha_{retro} &= \frac{2M}{b} \left(\sqrt{1-b^2u_R^2} + \sqrt{1-b^2u_S^2} \right) \\
&\quad + \frac{2aM}{b^2} \left(\sqrt{1-b^2u_R^2} + \sqrt{1-b^2u_S^2} \right) + \mathcal{O}\left(\frac{M^2}{b^2}\right). \tag{3.30}
\end{aligned}$$

Next, let us substitute Eqs.(3.18) and (3.21) into Eq.(2.52), then the bending angle of light for the prograde case is obtained as

$$\begin{aligned}
\alpha_{prog} &= \frac{2M}{b} \left(\sqrt{1-b^2u_R^2} + \sqrt{1-b^2u_S^2} \right) \\
&\quad - \frac{2aM}{b^2} \left(\sqrt{1-b^2u_R^2} + \sqrt{1-b^2u_S^2} \right) + \mathcal{O}\left(\frac{M^2}{b^2}\right), \tag{3.31}
\end{aligned}$$

and the bending angle for the retrograde case is

$$\begin{aligned}
\alpha_{retro} &= \frac{2M}{b} \left(\sqrt{1-b^2u_R^2} + \sqrt{1-b^2u_S^2} \right) \\
&\quad + \frac{2aM}{b^2} \left(\sqrt{1-b^2u_R^2} + \sqrt{1-b^2u_S^2} \right) + \mathcal{O}\left(\frac{M^2}{b^2}\right). \tag{3.32}
\end{aligned}$$

Note that a^2 terms at the second order in the bending angle from Eq.(2.51) cancel out because of Eq.(2.52). $\sqrt{1-b^2u_R^2}$ and $\sqrt{1-b^2u_S^2}$ parts in Eqs.(3.31) and (3.32) are real numbers, since it is ensured that $bu_R, bu_S < 1$ from the note after Eq.(3.15) in the preceding section.

For both cases, we take the far limit as $u_R \rightarrow 0$ and $u_S \rightarrow 0$. Then, we obtain

$$\alpha_{\infty prog} \rightarrow \frac{4M}{b} - \frac{4aM}{b^2} + O\left(\frac{M^2}{b^2}\right), \quad (3.33)$$

$$\alpha_{\infty retro} \rightarrow \frac{4M}{b} + \frac{4aM}{b^2} + O\left(\frac{M^2}{b^2}\right), \quad (3.34)$$

which shows that Eqs. (3.29) and (3.30) recover the asymptotic bending angles that are known in the literature [48–51].

comment: If readers wish to consider the bending angle of light in a case where the receiver point is closer to the source point than the closest approach point, Eqs.(3.29) and (3.30) become

$$\begin{aligned} \alpha_{prog} &= \frac{2M}{b} \left(\sqrt{1-b^2u_S^2} - \sqrt{1-b^2u_R^2} \right) \\ &\quad - \frac{2aM}{b^2} \left(\sqrt{1-b^2u_S^2} - \sqrt{1-b^2u_R^2} \right) + \mathcal{O}\left(\frac{M^2}{b^2}\right), \\ \alpha_{retro} &= \frac{2M}{b} \left(\sqrt{1-b^2u_S^2} - \sqrt{1-b^2u_R^2} \right) \\ &\quad + \frac{2aM}{b^2} \left(\sqrt{1-b^2u_S^2} - \sqrt{1-b^2u_R^2} \right) + \mathcal{O}\left(\frac{M^2}{b^2}\right). \end{aligned}$$

If reader wish to consider the bending angle of light in such a case that the source point is closer to the receiver than the closest approach point,

Eqs.(3.29) and (3.30) become

$$\begin{aligned}\alpha_{prog} &= \frac{2M}{b} \left(\sqrt{1 - b^2 u_R^2} - \sqrt{1 - b^2 u_S^2} \right) \\ &\quad - \frac{2aM}{b^2} \left(\sqrt{1 - b^2 u_R^2} - \sqrt{1 - b^2 u_S^2} \right) + \mathcal{O} \left(\frac{M^2}{b^2} \right), \\ \alpha_{retro} &= \frac{2M}{b} \left(\sqrt{1 - b^2 u_R^2} - \sqrt{1 - b^2 u_S^2} \right) \\ &\quad + \frac{2aM}{b^2} \left(\sqrt{1 - b^2 u_R^2} - \sqrt{1 - b^2 u_S^2} \right) + \mathcal{O} \left(\frac{M^2}{b^2} \right).\end{aligned}$$

3.7 Finite-distance corrections to the gravitomagnetic bending angle of light

The above sections discussed the bending angle of light due to the rotation of the lens (its spin parameter a). In particular, we did not assume that the receiver and the source were located at the infinity. The finite-distance correction to the bending angle of light, denoted as $\delta\alpha$, is the difference between the asymptotic bending angle α_∞ and the bending angle for the finite distance case. It is expressed as

$$\delta\alpha \equiv \alpha - \alpha_\infty. \quad (3.35)$$

Equations (3.29) and (3.30) suggest the magnitude of the finite-distance correction to the gravitomagnetic bending angle due to the spin as

$$\begin{aligned}|\delta\alpha_{GM}| &\sim O \left(\frac{aM}{r_S^2} + \frac{aM}{r_R^2} \right) \\ &\sim O \left(\frac{J}{r_S^2} + \frac{J}{r_R^2} \right),\end{aligned} \quad (3.36)$$

where we assumed $bu_R, bu_S < 1$, $J \equiv aM$ is the spin angular momentum of the lens and the subscript GM denotes the gravitomagnetic part. As usual, we introduce the dimensionless spin parameter as $s \equiv a/M$. Hence, Eq. (3.36) is rewritten as

$$|\delta\alpha_{GM}| \sim O\left(s\left(\frac{M}{r_S}\right)^2 + s\left(\frac{M}{r_R}\right)^2\right). \quad (3.37)$$

This suggests that $\delta\alpha_{GM}$ is comparable to the second post-Newtonian effect (multiplied by the dimensionless spin parameter).

It is known that the second-order Schwarzschild contribution to α is $15\pi M^2/4b^2$. This contribution can be found also by using the present method, especially when calculating ϕ_{RS} , we note a relation between b and r_0 in M^2 . See Appendix A for detailed calculations at the second order of M and a , especially the integrals of K and κ_g in the present formulation.

Note that $\delta\alpha_{GM}$ under the above approximations does not depend on the impact parameter b . In fact, we can check it from Figure 3.1 and Figure 3.4 of next section.

3.8 Possible astronomical applications

We discuss possible astronomical applications. First, we consider the Sun, where we ignore its higher multipole moments. The spin angular momentum of the Sun J_\odot is $\sim 2 \times 10^{41} \text{ m}^2 \text{ kg s}^{-1}$ [52]. Thus, $GJ_\odot c^{-2} \sim 5 \times 10^5 \text{ m}^2$, which implies the dimensionless spin parameter as $s_\odot \sim 10^{-1}$.

We assume that an observer at the Earth sees the light bent by the solar mass, while the source is practically at the asymptotic region. If the light ray passes near the solar surface, Eq. (3.37) implies that the finite-distance

correction to this case is of the order of

$$\begin{aligned}
|\delta\alpha_{GM}| &\sim O\left(\frac{J}{r_R^2}\right) \\
&\sim 10^{-12}\text{arcsec.} \times \left(\frac{J}{J_\odot}\right) \left(\frac{1\text{AU}}{r_R}\right)^2, \tag{3.38}
\end{aligned}$$

where $4M_\odot/R_\odot \sim 1.75 \text{ arcsec.} \sim 10^{-5} \text{ rad.}$, M_{\odot} denotes the solar mass and R_\odot denotes the solar radius. This correction is around a pico-arcsecond level and thus it is unlikely to be observed with present and future technology [53, 54].

See Figure 3.1 for the numerical calculations of the finite-distance correction due to the receiver location. The numerical results are consistent with the above order-of-magnitude estimation. The figure suggests that the dependence of $\delta\alpha$ on the impact parameter b is very weak.

See Figures 3.2 and 3.3 for the numerical calculations of the bending angle with finite-distance corrections for prograde motion and retrograde motion, respectively, due to the impact parameter b . We have chosen $r_S \sim 1.5 \times 10^8 \text{ km}$ and $r_R \sim \infty$. This suggests that the finite-distance correction reduces the bending angle. As the impact parameter b increases, the finite-distance correction also increases.

Next, we consider Sgr A* at the center of our Galaxy, which is expected as one of the most plausible candidates for the strong deflection of light. In this case, the receiver distance is much larger than the impact parameter of light, while a source star may be in the central region of our Galaxy.

For Sgr A*, Eq. (3.36) implies

$$\begin{aligned}
|\delta\alpha_{GM}| &\sim s \left(\frac{M}{r_S}\right)^2 \\
&\sim 10^{-7}\text{arcsec.} \times \left(\frac{s}{0.1}\right) \left(\frac{M}{4 \times 10^6 M_\odot}\right)^2 \left(\frac{0.1\text{pc}}{r_S}\right)^2, \tag{3.39}
\end{aligned}$$

where we assumed the mass of the central black hole as $M \sim 4 \times 10^6 M_\odot$. This correction around a sub-microarcsecond level is unlikely to be measured with present technology.

See Figure 3.4 for the numerical calculations of the finite-distance correction due to the source location. The numerical results are consistent with the above order-of-magnitude estimation. The figure shows that the dependence on the impact parameter b is very weak.

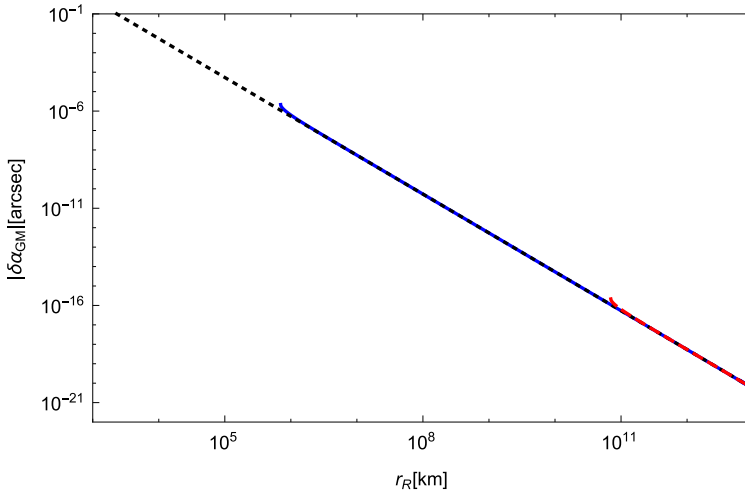


Figure 3.1: $\delta\alpha_{GM}$ for the Sun. The vertical axis denotes the finite-distance correction to the gravitomagnetic bending angle of light and the horizontal axis denotes the receiver distance r_R . The solid curve (blue in color) and dashed one (red in color) correspond to $b = R_\odot$ and $b = 10^5 R_\odot$, respectively. The dotted line (black in color) denotes the leading term in $\delta\alpha_{GM}$ given by Eq. (3.36). The overlap between these curves suggests that the dependence of $\delta\alpha_{GM}$ on the impact parameter b is very weak.

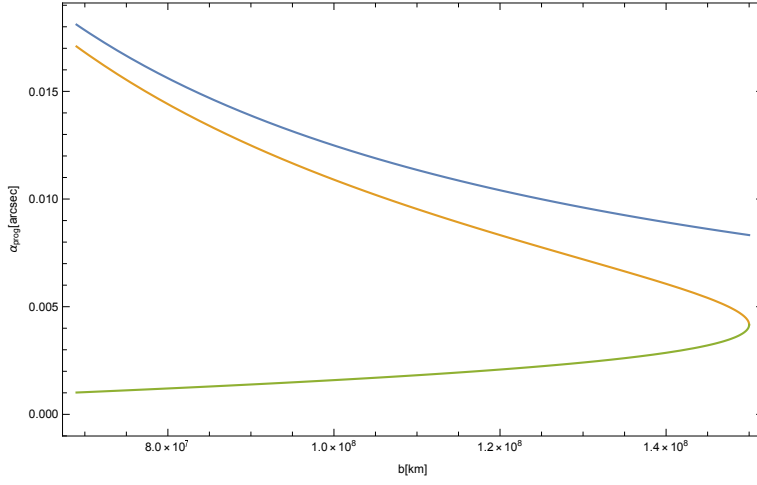


Figure 3.2: The bending angle for light of prograde motion. The horizontal axis denotes the impact parameter for a photon orbit and the vertical axis denotes the bending angle of light. The blue curve is the asymptotic bending angle by a Kerr black hole. The orange curve is the bending angle with finite-correction by a Kerr black hole. The green curve shows the difference between the asymptotic bending angle and the bending angle with finite-correction by a Kerr black hole.

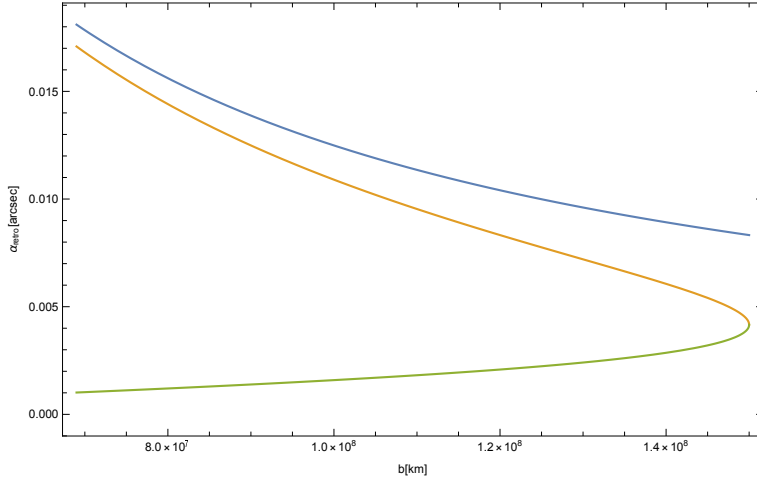


Figure 3.3: The bending angle for light of retrograde motion. The horizontal axis denotes the impact parameter for a photon orbit and the vertical axis denotes the bending angle of light. The blue curve is the asymptotic bending angle by the Kerr black hole. The orange curve is the bending angle with finite-correction by the Kerr black hole. The green curve shows the difference between the asymptotic bending angle and the bending angle with finite-correction by the Kerr black hole.

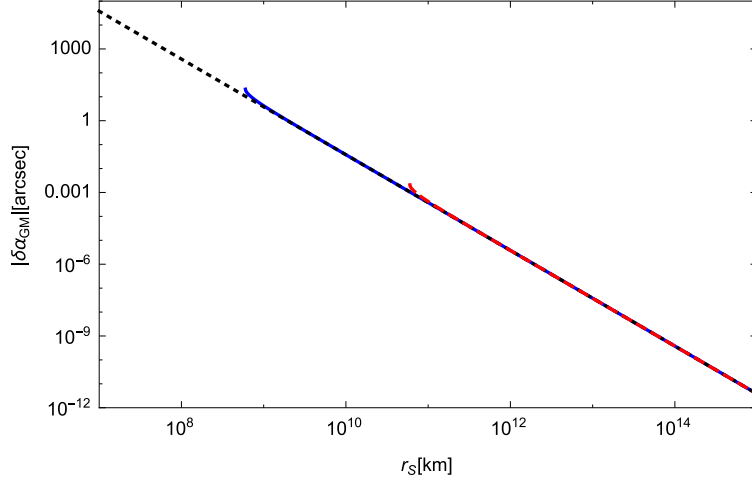


Figure 3.4: $\delta\alpha_{GM}$ for Sgr A*. The vertical axis denotes the finite-distance correction to the bending angle of light and the horizontal axis denotes the source distance r_S . The solid curve (blue in color) and dashed one (red in color) correspond to $b = 10^2 M$ and $b = 10^4 M$, respectively. The dotted line (yellow in color) denotes the leading term in $\delta\alpha_{GM}$ given by Eq. (3.36). The overlap between these plots suggests that $\delta\alpha_{GM}$ depends faintly on the impact parameter b .

Chapter 4

Application to rotating Teo wormhole

4.1 Rotating Teo wormhole and optical metric

In this section, we consider a rotating Teo wormhole [55] in order to confirm whether our method could compute for a wormhole spacetime. Its spacetime metric reads

$$ds^2 = -N^2 dt^2 + \frac{dr^2}{1 - \frac{b_0}{r}} + r^2 H^2 \left[d\theta^2 + \sin^2 \theta (d\phi - \omega dt)^2 \right], \quad (4.1)$$

where

$$N = H = 1 + \frac{d(4\bar{a} \cos \theta)^2}{r}, \quad (4.2)$$

$$\omega = \frac{2\bar{a}}{r^3}. \quad (4.3)$$

Here, b_0 denotes the throat radius of this wormhole, \bar{a} corresponds to the spin angular momentum, and d is a positive constant.

For the rotating Teo wormhole Eq.(4.1), we find the components of the generalized optical metric as

$$\begin{aligned} \gamma_{ij}dx^i dx^j = & \frac{r^7}{(r - b_0) (r^4 - 4\bar{a}^2 \sin^2 \theta) (16d\bar{a}^2 \cos^2 \theta + r)^2} dr^2 \\ & + \frac{r^6}{r^4 - 4\bar{a}^2 \sin^2 \theta} d\theta^2 + \frac{r^{10} \sin^2 \theta}{(r^4 - 4\bar{a}^2 \sin^2 \theta)^2} d\phi^2. \end{aligned} \quad (4.4)$$

Note that γ_{ij} is not the induced metric in the ADM (Arnowitt-Deser-Misner) formalism. We obtain the components of β_i as

$$\beta_i dx^i = - \frac{2\bar{a}r^3 \sin^2 \theta}{r^4 - 4\bar{a}^2 \sin^2 \theta} d\phi. \quad (4.5)$$

In this thesis, we focus on the light rays in the equatorial plane, namely $\theta = \pi/2$. Then, the constant d in the metric does not appear because d is coupling to $\cos \theta$.

As with the Kerr case, we first consider the orbit equation on the equatorial plane from Eq.(2.41) as

$$\begin{aligned} \left(\frac{dr}{d\phi} \right)^2 &= - \frac{r^5(b_0 - r) (4\bar{a}^2 b^2 - 4\bar{a}br^3 - b^2 r^4 + r^6)}{(-4\bar{a}^2 b + 2\bar{a}r^3 + br^4)^2} \\ &= \frac{r^4}{b^2} - r^2 - \frac{b_0 r^3}{b^2} + b_0 r - \frac{4\bar{a}r^3}{b^3} + \frac{4\bar{a}b_0 r^2}{b^3} + \mathcal{O}(\bar{a}^2/b^2), \end{aligned} \quad (4.6)$$

where b is the impact parameter of the photon and we used the weak field and slow rotation approximations in the last line. There are no b_0 squared in the last line. The orbit equation in this case becomes

$$\left(\frac{du}{d\phi} \right)^2 = \frac{1}{b^2} - u^2 - \frac{b_0 u}{b^2} + b_0 u^3 - \frac{4\bar{a}u}{b^3} - \frac{4\bar{a}b_0 u^2}{b^3} + \mathcal{O}(\bar{a}^2/b^6). \quad (4.7)$$

This is iteratively solved as

$$u = \frac{\sin \phi}{b} + \frac{\cos^2 \phi}{2b^2} b_0 - \frac{2}{b^3} \bar{a} + \mathcal{O}\left(\frac{b_0^2}{b^3}, \frac{\bar{a}b_0}{b^4}\right). \quad (4.8)$$

Solving Eq.(4.8) for ϕ_S and ϕ_R , we obtain ϕ_S and ϕ_R as

$$\begin{aligned} \phi_S &= \arcsin(bu_S) - \frac{b_0\sqrt{1-b^2u_S^2}}{2b} + \frac{2\bar{a}}{b^2\sqrt{1-b^2u_S^2}} + \mathcal{O}\left(\frac{b_0^2}{b^2}, \frac{\bar{a}b_0}{b^3}\right), \\ \phi_R &= \pi - \arcsin(bu_R) + \frac{b_0\sqrt{1-b^2u_R^2}}{2b} - \frac{2\bar{a}}{b^2\sqrt{1-b^2u_R^2}} + \mathcal{O}\left(\frac{b_0^2}{b^2}, \frac{\bar{a}b_0}{b^3}\right). \end{aligned} \quad (4.10)$$

4.2 Gaussian curvature

For the equatorial case of a rotating Teo wormhole, the Gaussian curvature in the weak field approximation is calculated as

$$\begin{aligned} K &= \frac{R_{r\phi r\phi}}{\det \gamma} \\ &= \frac{1}{\sqrt{\det \gamma}} \left[\frac{\partial}{\partial \phi} \left(\frac{\sqrt{\det \gamma}}{\gamma_{rr}} {}^{(3)}\Gamma_{rr}^\phi \right) - \frac{\partial}{\partial r} \left(\frac{\sqrt{\det \gamma}}{\gamma_{rr}^{(3)}} \Gamma_{r\phi}^\phi \right) \right] \\ &= -\frac{b_0}{2r^3} - \frac{56\bar{a}^2}{r^6} + \mathcal{O}\left(\frac{\bar{a}^2b_0}{r^7}, \frac{\bar{a}^4}{r^{10}}\right), \end{aligned} \quad (4.11)$$

where γ denotes $\det(\gamma_{ij})$, and \bar{a} and b_0 are book-keeping parameters in the weak field approximation. It is not surprising that this Gaussian curvature does not agree with Eq. (26) in a paper by Jusufi and Övgün [56], because their Gaussian curvature describes another surface that is associated with the Randers-Finsler metric different from our generalized optical metric γ_{ij} .

In order to perform the surface integral of the Gaussian curvature in Eq. (2.52), we use Eq.(4.8) as the boundary of the integration domain. The

surface integral of the Gaussian curvature in Eq. (2.52) is calculated as

$$\begin{aligned}
-\iint_{\infty_R \square_S^\infty} K dS &= \int_{\phi_S}^{\phi_R} \int_{\infty}^{r(\phi)} \left(-\frac{b_0}{2r^2} \right) dr d\phi + \mathcal{O}\left(\frac{b_0^2}{b^2}, \frac{\bar{a}b_0}{b^3}\right) \\
&= \frac{b_0}{2} \int_{\phi_S}^{\phi_R} \int_0^{\frac{\sin \phi}{b} + \frac{\cos^2 \phi}{2b^2} b_0 - \frac{2}{b^3} \bar{a}} du d\phi + \mathcal{O}\left(\frac{b_0^2}{b^2}, \frac{\bar{a}b_0}{b^3}\right) \\
&= \frac{b_0}{2} \int_{\phi_S}^{\phi_R} \left[\frac{\sin \phi}{b} \right] d\phi + \mathcal{O}\left(\frac{b_0^2}{b^2}, \frac{\bar{a}b_0}{b^3}\right) \\
&= \frac{b_0}{2} \left[-\frac{\cos \phi}{b} \right]_{\phi=\phi_S}^{\phi_R} + \mathcal{O}\left(\frac{b_0^2}{b^2}, \frac{\bar{a}b_0}{b^3}\right) \\
&= \frac{b_0}{2b} \left(\sqrt{1 - b^2 u_R^2} + \sqrt{1 - b^2 u_S^2} \right) + \mathcal{O}\left(\frac{b_0^2}{b^2}, \frac{\bar{a}b_0}{b^3}\right), \quad (4.12)
\end{aligned}$$

where we used $\sin \phi_R = bu_R + \mathcal{O}(\bar{a}b^{-2}, b_0b^{-1})$ and $\sin \phi_S = bu_S + \mathcal{O}(\bar{a}b^{-2}, b_0b^{-1})$ by Eqs.(4.10) and (4.9) in the last line.

4.3 Geodesic curvature of photon orbit

On the equatorial plane in the stationary and axisymmetric spacetime, the geodesic curvature of the photon orbit with the generalized optical metric becomes [57]

$$\kappa_g = -\sqrt{\frac{1}{\gamma\gamma_{\theta\theta}}} \beta_{\phi,r}. \quad (4.13)$$

For the Teo wormhole case, this is obtained as

$$\kappa_g = -\frac{2\bar{a}}{r^3} + \frac{\bar{a}b_0}{r^4} + \frac{\bar{a}b_0^2}{4r^5} + \frac{\bar{a}b_0^3}{8r^6} + \mathcal{O}\left(\frac{\bar{a}^3}{r^7}, \frac{\bar{a}^3b_0}{r^8}\right). \quad (4.14)$$

We examine the contribution from the geodesic curvature. This contribution is the path integral along the photon orbit from the source to the

receiver, which is computed as

$$\begin{aligned}
\int_S^R \kappa_g d\ell &= \int_R^S \frac{2\bar{a}}{r^3} d\ell + \mathcal{O}\left(\frac{b_0^2}{b^2}, \frac{\bar{a}b_0}{b^3}\right) \\
&= \int_{\pi/2-\phi_R}^{\pi/2-\phi_S} \frac{2\bar{a} \cos \vartheta}{b^2} d\vartheta + \mathcal{O}\left(\frac{b_0^2}{b^2}, \frac{\bar{a}b_0}{b^3}\right) \\
&= \frac{2\bar{a}}{b^2} \left[\sin\left(\frac{\pi}{2} - \phi_S\right) - \sin\left(\frac{\pi}{2} - \phi_R\right) \right] + \mathcal{O}\left(\frac{b_0^2}{b^2}, \frac{\bar{a}b_0}{b^3}\right) \\
&= \frac{2\bar{a}}{b^2} \left(\sqrt{1 - b^2 u_S^2} + \sqrt{1 - b^2 u_R^2} \right) + \mathcal{O}\left(\frac{b_0^2}{b^2}, \frac{\bar{a}b_0}{b^3}\right), \quad (4.15)
\end{aligned}$$

for the retrograde case of the photon orbit. In the last line, we used $\sin \phi_R = bu_R + \mathcal{O}(\bar{a}b^{-2}, b_0b^{-1})$ and $\sin \phi_S = bu_S + \mathcal{O}(\bar{a}b^{-2}, b_0b^{-1})$ from Eq. (4.8). The above contribution becomes $4\bar{a}/b^2$, as $r_R \rightarrow \infty$ and $r_S \rightarrow \infty$. The sign of the right hand side of Eq. (4.15) changes, if the photon orbit is prograde.

4.4 ϕ_{RS} part

We notice that the rotating Teo wormhole is an asymptotically flat space-time, from Eq.(4.1). Therefore, the integral of the geodesic curvature of the circular arc segment with an infinite radius can be rewritten as ϕ_{RS} . By using Eqs.(4.9) and (4.10), we obtain ϕ_{RS} as

$$\begin{aligned}
\phi_{RS} &= \phi_R - \phi_S \\
&= \pi - \arcsin(bu_R) - \arcsin(bu_S) + \frac{b_0\sqrt{1 - b^2 u_R^2}}{2b} + \frac{b_0\sqrt{1 - b^2 u_S^2}}{2b} \\
&\quad - \frac{2\bar{a}}{b^2\sqrt{1 - b^2 u_R^2}} - \frac{2\bar{a}}{b^2\sqrt{1 - b^2 u_S^2}} + \mathcal{O}\left(\frac{b_0^2}{b^2}, \frac{\bar{a}b_0}{b^3}\right). \quad (4.16)
\end{aligned}$$

4.5 Ψ parts

For the rotating Teo wormhole metric by Eq.(4.1), Eq.(2.49) is obtained as

$$\sin \Psi_R = bu_R + 2\bar{a}u_R^2 - 4\bar{a}^2bu_R^5, \quad (4.17)$$

and Eq.(2.50) becomes

$$\sin(\pi - \Psi_S) = bu_S + 2\bar{a}u_S^2 - 4\bar{a}^2bu_S^5, \quad (4.18)$$

where we do not use the slow rotation approximation. Therefore, Ψ_R and Ψ_S are obtained as

$$\Psi_R = \arcsin(bu_R) + \frac{2\bar{a}u_R^2}{\sqrt{1 - b^2u_R^2}} + \frac{2\bar{a}^2bu_R^5(2b^2u_R^2 - 1)}{(b^2u_R^2 - 1)^{3/2}} + \mathcal{O}(\bar{a}^3/b^6), \quad (4.19)$$

$$\pi - \Psi_S = \arcsin(bu_S) + \frac{2\bar{a}u_S^2}{\sqrt{1 - b^2u_S^2}} + \frac{2\bar{a}^2bu_S^5(2b^2u_S^2 - 1)}{(b^2u_S^2 - 1)^{3/2}} + \mathcal{O}(\bar{a}^3/b^6), \quad (4.20)$$

where we used the slow rotation approximation.

4.6 Bending angle of light

By combining Eqs. (4.12) and (4.15), the bending angle of light for the prograde case is obtained as

$$\begin{aligned} \alpha_{\text{prog}} = & \frac{b_0}{2b} \left(\sqrt{1 - b^2u_R^2} + \sqrt{1 - b^2u_S^2} \right) - \frac{2\bar{a}}{b^2} \left(\sqrt{1 - b^2u_R^2} + \sqrt{1 - b^2u_S^2} \right) \\ & + \mathcal{O} \left(\frac{b_0^2}{b^2}, \frac{\bar{a}b_0}{b^3} \right). \end{aligned} \quad (4.21)$$

The bending angle for the retrograde case is

$$\alpha_{\text{retro}} = \frac{b_0}{2b} \left(\sqrt{1 - b^2 u_R^2} + \sqrt{1 - b^2 u_S^2} \right) + \frac{2\bar{a}}{b^2} \left(\sqrt{1 - b^2 u_R^2} + \sqrt{1 - b^2 u_S^2} \right) + \mathcal{O} \left(\frac{b_0^2}{b^2}, \frac{\bar{a}b_0}{b^3} \right). \quad (4.22)$$

Next, by using Eqs. (4.16), (4.19) and (4.20), the bending angle of light for the prograde case is obtained as

$$\begin{aligned} \alpha_{\text{prog}} &= \pi - \arcsin(bu_R) - \arcsin(bu_S) + \frac{b_0\sqrt{1 - b^2 u_R^2}}{2b} + \frac{b_0\sqrt{1 - b^2 u_S^2}}{2b} \\ &\quad - \frac{2\bar{a}}{b^2\sqrt{1 - b^2 u_R^2}} - \frac{2\bar{a}}{b^2\sqrt{1 - b^2 u_S^2}} + \arcsin(bu_R) + \frac{2\bar{a}u_R^2}{\sqrt{1 - b^2 u_R^2}} \\ &\quad - \pi + \arcsin(bu_S) + \frac{2\bar{a}u_S^2}{\sqrt{1 - b^2 u_S^2}} + \mathcal{O} \left(\frac{b_0^2}{b^2}, \frac{\bar{a}b_0}{b^3} \right) \\ &= \frac{b_0}{2b} \left(\sqrt{1 - b^2 u_R^2} + \sqrt{1 - b^2 u_S^2} \right) - \frac{2\bar{a}}{b^2} \left(\sqrt{1 - b^2 u_R^2} + \sqrt{1 - b^2 u_S^2} \right) \\ &\quad + \mathcal{O} \left(\frac{b_0^2}{b^2}, \frac{\bar{a}b_0}{b^3} \right). \end{aligned} \quad (4.23)$$

The bending angle for the retrograde case is

$$\alpha_{\text{retro}} = \frac{b_0}{2b} \left(\sqrt{1 - b^2 u_R^2} + \sqrt{1 - b^2 u_S^2} \right) + \frac{2\bar{a}}{b^2} \left(\sqrt{1 - b^2 u_R^2} + \sqrt{1 - b^2 u_S^2} \right) + \mathcal{O} \left(\frac{b_0^2}{b^2}, \frac{\bar{a}b_0}{b^3} \right). \quad (4.24)$$

The deflection of light in the prograde (retrograde) direction is decreasing (increasing) with increasing the angular momentum of the Teo wormhole, because the local inertial frame (in which the light propagates at the light speed c in general relativity) moves faster (slower), and hence the light ray feels the gravitational pull for shorter (longer) time. Regarding the light propagation around a rotating object, similar physical explanations based on the dragging of the inertial frame were done about the Shapiro time delay

by Laguna and Wolszczan [58]. The expression of the bending angle of light by a rotating Teo wormhole is similar to the bending angle by Kerr black hole. This suggests that it is difficult to distinguish between Kerr black hole and rotating Teo wormhole from observations of the gravitational lens.

For Eqs.(4.23) and (4.24), the source and receiver may be located at finite distance from the wormhole. One can see that, in the limit as $r_R \rightarrow \infty$ and $r_S \rightarrow \infty$, Eqs. (4.21) and (4.22) become

$$\begin{aligned}\alpha_{\text{prog}} &\rightarrow \frac{b_0}{b} - \frac{4\bar{a}}{b^2} + \mathcal{O}\left(\frac{b_0^2}{b^2}, \frac{\bar{a}b_0}{b^3}\right), \\ \alpha_{\text{retro}} &\rightarrow \frac{b_0}{b} + \frac{4\bar{a}}{b^2} + \mathcal{O}\left(\frac{b_0^2}{b^2}, \frac{\bar{a}b_0}{b^3}\right).\end{aligned}\tag{4.25}$$

They agree with Eqs. (39) and (56) in Jusufi and Övgün [56], in which they are restricted within the asymptotic source and receiver ($r_R \rightarrow \infty$ and $r_S \rightarrow \infty$).

4.7 Finite-distance corrections to the bending angle of light

The finite-distance correction to the bending angle of light, denoted as $\delta\alpha$, is the difference between the asymptotic bending angle α_∞ and the asymptotic bending angle.

We assume that an observer at the Earth sees the light bending by the solar mass, while the source is practically at the asymptotic region. In other words, we have chosen $b_0 = M_\odot$, $\bar{a} = J_\odot$, $r_R \sim 1.5 \times 10^8$ km, $r_S \sim \infty$. See Figure 4.1 for numerical calculations of the finite-distance correction due to the impact parameter b . In figure 4.1, the green curve is the difference between the asymptotic bending angle and the bending angle with finite-correction, the blue curve is the asymptotic bending angle and the orange

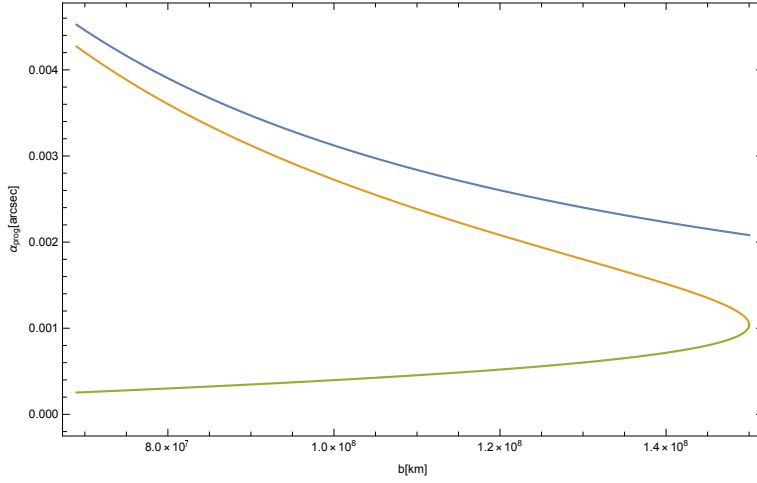


Figure 4.1: The blue curve is the asymptotic bending angle with finite-correction by the rotating Teo wormhole. The vertical axis denotes the The orange curve is the bending angle with finite-correction by the rotating Teo wormhole. The blue curve shows the difference between the asymptotic bending angle and the bending angle with finite-correction by the rotating Teo wormhole.

curve is the bending angle with finite-correction by the rotating Teo wormhole. This suggests that the finite-distance correction reduces the bending angle. As the impact parameter b increases, the finite-distance correction also increases.

See Figure 4.2 for numerical calculations of the finite-distance correction due to the impact parameter b . In Figure 4.2, the blue curve is the bending angle with finite-distance correction by a Kerr black hole and the red curve is the bending angle with finite-correction by a rotating Teo wormhole. This suggests that the bending of light is stronger in a Kerr black hole case for the chosen values.

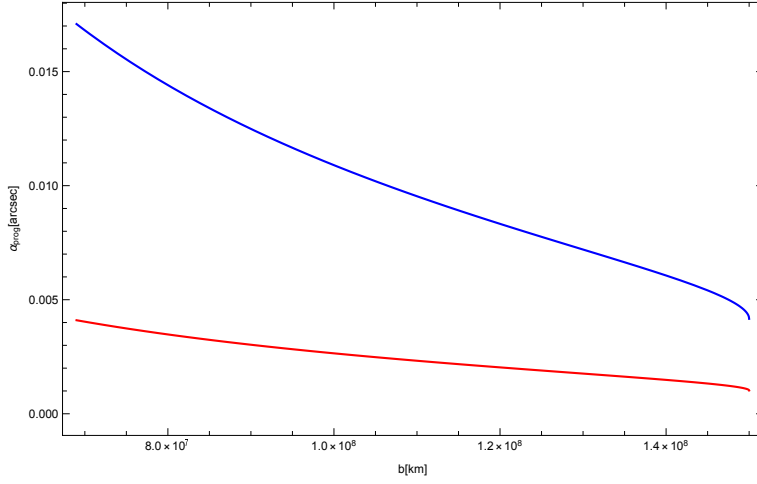


Figure 4.2: The bending angle for prograde motion of light. The horizontal axis denotes the impact parameter of photon orbit and the vertical axis denotes the bending angle of light. The blue curve is the bending angle with finite-distance correction by the Kerr black hole. The red curve is the bending angle with finite-correction by the rotating Teo wormhole. The Mass of a Kerr black hole M and the throat radius of a rotating Teo wormhole b_0 are $M = b_0 = M_{\odot}$. The spin angular momentum of a Kerr black hole and the spin angular momentum of a rotating Teo wormhole are the spin angular momentum of the Sun.

Chapter 5

Conclusion

By using the Gauss-Bonnet theorem in differential geometry, we discussed a possible extension of the method of calculating the bending angle of light to stationary, axisymmetric and asymptotically flat spacetimes. Instead of using Randers-Finsler metric, we introduced a generalized optical metric γ_{ij} to define the bending angle of light, which was shown to be coordinate-invariant. We considered the light rays on the equatorial plane in the axisymmetric spacetime. On the analogy of the thin lens approximation, we defined the bending angle of light

$$\alpha = \Psi_R - \Psi_S + \phi_{RS}. \quad (5.1)$$

By using the Gauss-Bonnet theorem, it is rewritten as

$$\alpha = - \iint_{\infty_R \square_S^\infty} K dS - \int_R^S \kappa_g d\ell. \quad (5.2)$$

Our definition of the bending angle corresponds to an extension of the bending angle in the thin lens approximation, especially by taking account of the curved space and the singularity at the lens point. We showed that the

geodesic curvature κ_g of the photon orbit can be nonzero in gravitomagnetism, even though the light ray in the four-dimensional spacetime follows the null geodesic. We considered Kerr spacetime and the rotating Teo wormhole, in order to demonstrate how the bending angle of light is computed by the present method. By using the results in the Kerr case, we made an order-of-magnitude estimate of the finite-distance corrections for two possible astronomical cases; (1) the Sun and (2) the Sgr A*. The dependence of the magnitude of the finite-distance correction to the gravitomagnetic bending angle on the impact parameter b was quite weak. These results suggest that the finite-distance corrections due to gravitomagnetism are unlikely to be observed with present technology.

By using the results in the rotating Teo wormhole, it is interesting to compare the finite-distance corrections of the bending angle by the rotating Teo wormhole with Kerr black hole. The finite-distance corrections had the same form and it reduces the bending angle. As the impact parameter b increases the finite-distance correction also increases.

However, our analysis on possible astronomical observations in this paper was limited within the Kerr model and rotating Teo wormhole. It might be interesting to examine the gravitomagnetic bending of light by using other axisymmetric spacetimes in general relativity or in a specific theory of modified gravity [60–67]. A further study along this direction is left for future. It would be interesting to study an extension of the formulation of gravitational lensing, Eqs.(B.2) \sim (B.8) to a finite-distance situation. See Appendix B for more details.

Appendix A

Detailed calculations of the bending angle by a Kerr black hole at $O(M^2/b^2)$ and $O(a^2/b^2)$

First, we consider K given by Eq.(3.16). Up to the second order, it is expanded as

$$\begin{aligned} K &= \frac{R_{r\phi r\phi}}{\det \gamma_{ij}^{(2)}} \\ &= -\frac{2M}{r^3} + \frac{3M^2}{r^4} + \mathcal{O}\left(\frac{a^2 M}{r^5}\right). \end{aligned} \tag{A.1}$$

Note that there are no a^2 terms in K . More interestingly, only the $a^2 M$ term among the third order terms do exist in K . We notice what we need for the second-order calculations is only the linear order in the area element on the equatorial plane, by noting that K begins with $\mathcal{O}(M)$. The area element on

the equatorial plane is thus obtained as

$$\begin{aligned} dS &\equiv \sqrt{\det \gamma_{ij}^{(2)}} dr d\phi \\ &= \left[r + 3M + \mathcal{O}\left(\frac{M^2}{r}\right) \right] dr d\phi, \end{aligned} \tag{A.2}$$

where terms at $\mathcal{O}(a)$ and also at $\mathcal{O}(a^2/r)$ do not exist in dS . This is because all terms including the spin parameter cancel out in $\det \gamma_{ij}^{(2)}$ for $\theta = \pi/2$ and $\det \gamma_{ij}^{(2)}$ thus depends only on M , as can be shown by direct calculations.

By using Eqs. (A.1) and (A.2), the surface integration of the Gaussian

curvature is done as

$$\begin{aligned}
- \iint_{\int_R^{\infty} \square_S^{\infty}} K dS &= \int_{\phi_S}^{\phi_R} \int_{\infty}^{r_{OE}} \left(-\frac{2M}{r^3} + \frac{3M^2}{r^4} \right) (r + 3M) dr d\phi + \mathcal{O} \left(\frac{M^3}{b^3}, \frac{aM^2}{b^3}, \frac{a^2M}{b^3} \right) \\
&= \int_{\phi_S}^{\phi_R} \int_0^{\frac{1}{b} \sin \phi + \frac{M}{b^2} (1 + \cos^2 \phi)} (2M + 3uM^2) du d\phi + \mathcal{O} \left(\frac{M^3}{b^3}, \frac{aM^2}{b^3}, \frac{a^2M}{b^3} \right) \\
&= \int_{\phi_S}^{\phi_R} \left[2uM + \frac{3u^2}{2} M^2 \right]_0^{\frac{1}{b} \sin \phi + \frac{M}{b^2} (1 + \cos^2 \phi)} d\phi + \mathcal{O} \left(\frac{M^3}{b^3}, \frac{aM^2}{b^3}, \frac{a^2M}{b^3} \right) \\
&= \int_{\phi_S}^{\phi_R} \left[\frac{2M}{b} \sin \phi + \frac{M^2}{2b^2} (7 + \cos^2 \phi) \right] d\phi + \mathcal{O} \left(\frac{M^3}{b^3}, \frac{aM^2}{b^3}, \frac{a^2M}{b^3} \right) \\
&= \frac{2M}{b} \left[\cos \phi \right]_{\phi_R}^{\phi_S} + \frac{M^2}{2b^2} \left[\frac{30\phi + \sin(2\phi)}{4} \right]_{\phi_S}^{\phi_R} + \mathcal{O} \left(\frac{M^3}{b^3}, \frac{aM^2}{b^3}, \frac{a^2M}{b^3} \right) \\
&= \frac{2M}{b} \left[\sqrt{1 - b^2 u_S^2} + \sqrt{1 - b^2 u_R^2} \right] \\
&\quad + \frac{2M^2}{b} \left[\frac{u_S(2 - b^2 u_S^2)}{\sqrt{1 - b^2 u_S^2}} + \frac{u_R(2 - b^2 u_R^2)}{\sqrt{1 - b^2 u_R^2}} \right] \\
&\quad + \frac{15M^2}{4b^2} [\pi - \arcsin(bu_S) - \arcsin(bu_R)] \\
&\quad - \frac{M^2}{4b^2} [bu_S \sqrt{1 - b^2 u_S^2} + bu_R \sqrt{1 - b^2 u_R^2}] + \mathcal{O} \left(\frac{M^3}{b^3}, \frac{aM^2}{b^3}, \frac{a^2M}{b^3} \right) \\
&= \frac{2M}{b} \left[\sqrt{1 - b^2 u_S^2} + \sqrt{1 - b^2 u_R^2} \right] \\
&\quad + \frac{15M^2}{4b^2} [\pi - \arcsin(bu_S) - \arcsin(bu_R)] \\
&\quad + \frac{M^2}{4b^2} \left[\frac{bu_S(15 - 7b^2 u_S^2)}{\sqrt{1 - b^2 u_S^2}} + \frac{bu_R(15 - 7b^2 u_R^2)}{\sqrt{1 - b^2 u_R^2}} \right] \\
&\quad + \mathcal{O} \left(\frac{M^3}{b^3}, \frac{aM^2}{b^3}, \frac{a^2M}{b^3} \right), \tag{A.3}
\end{aligned}$$

where we used, in the second line, an iterative solution for the orbit equation given by Eq. (3.14) for the Kerr spacetime.

Next, we study the geodesic curvature. On the equatorial plane, we obtain

$$\begin{aligned}\kappa_g &= - \frac{1}{\sqrt{\frac{\Sigma^2}{\Delta(\Sigma - 2Mr)} \left(r^2 + a^2 + \frac{2a^2 Mr \sin^2 \theta}{\Sigma} \right) \frac{\Sigma \sin^2 \theta}{(\Sigma - 2Mr)}}} \beta_{\phi, r} \\ &= - \frac{2aM}{r^3} + O\left(\frac{aM^2}{r^3}\right),\end{aligned}\tag{A.4}$$

where a^2 terms do not exist. From this, we obtain

$$\begin{aligned}- \int_R^S \kappa_g d\ell &= - \int_S^R \frac{2aM}{r^3} d\ell \\ &= - \frac{2aM}{b^2} \int_{\phi_S}^{\phi_R} \sin \phi d\phi \\ &= - \frac{2aM}{b^2} [\cos \phi_S - \cos \phi_R] \\ &= - \frac{2aM}{b^2} [\sqrt{1 - b^2 u_R^2} + \sqrt{1 - b^2 u_S^2}],\end{aligned}\tag{A.5}$$

where we used $\cos \phi_S = \sqrt{1 - b^2 u_S^2} + O(Mu_S)$ and $\cos \phi_R = -\sqrt{1 - b^2 u_R^2} + O(Mu_R)$.

By combining Eqs. (A.3) and (A.5), we obtain

$$\begin{aligned}\alpha &\equiv - \iint_{\infty_R \square \infty_S} K dS - \int_R^S \kappa_g d\ell \\ &= \frac{2M}{b} [\sqrt{1 - b^2 u_S^2} + \sqrt{1 - b^2 u_R^2}] \\ &\quad + \frac{15M^2}{4b^2} [\pi - \arcsin(bu_S) - \arcsin(bu_R)] \\ &\quad + \frac{M^2}{4b^2} \left[\frac{bu_S(15 - 7b^2 u_S^2)}{\sqrt{1 - b^2 u_S^2}} + \frac{bu_R(15 - 7b^2 u_R^2)}{\sqrt{1 - b^2 u_R^2}} \right] \\ &\quad - \frac{2aM}{b^2} [\sqrt{1 - b^2 u_R^2} + \sqrt{1 - b^2 u_S^2}] + O\left(\frac{M^3}{b^3}, \frac{aM^2}{b^3}, \frac{a^2 M}{b^3}\right).\end{aligned}\tag{A.6}$$

Note that a^2 terms and a^3 ones do not appear in α for the finite distance situation as well as in the infinite distance limit. If we assume the infinite distance limit $u_R, u_S \rightarrow 0$, Eq. (A.6) becomes

$$\alpha \rightarrow \frac{4M}{b} + \frac{15\pi M^2}{4b^2} - \frac{4aM}{b^2}, \quad (\text{A.7})$$

where we use $\arcsin(bu_R) \rightarrow \pi$ and $\arcsin(bu_S) \rightarrow 0$. This agrees with the previous results in Ref. [48–51], especially with the numerical coefficients at the order of M^2 and aM .

Appendix B

Relation to the lens equation, the magnitude etc.

In general relativity, gravity is able to deflect light like Figure B.1. When the light passes from the source to the receiver, there can be multiple routes because of deflection of light. Therefore, we can see multiple images due to the existence of matter which is between the light source and the observer. Such a region of mass concentration or mass object is called a gravitational lens. Gravitational lens effect is one of the important means of astronomy. Information on the large-scale structure of the universe can be obtained through the gravitational lens effect if the distance from the source to lens object, the distance from the source to the receiver and the distance from the lens to the receiver are all cosmological scales.

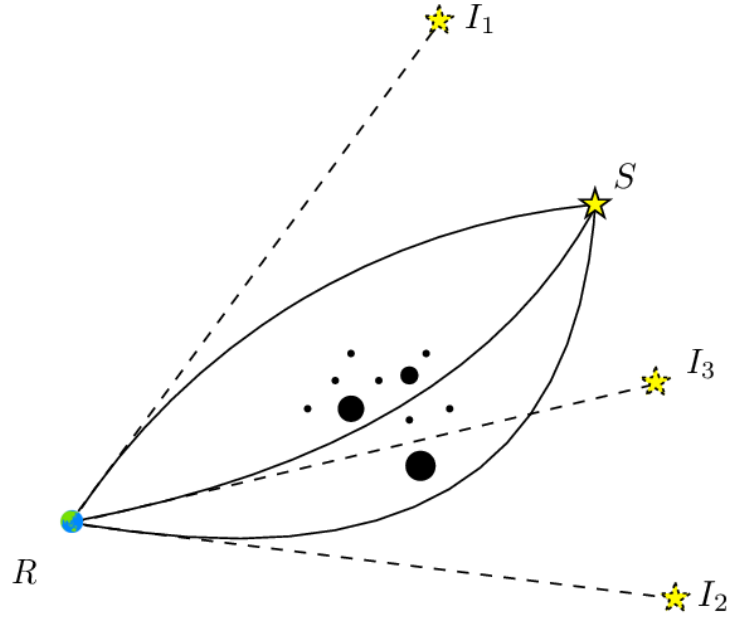


Figure B.1: Schematic figure for the gravitational lens. Since the light ray from the source S is bent by the distribution of mass which exists between the source and the receiver R , multiple paths light rays are made between the light source and the receiver.

Bending angle and Lens equation:

On the assumptions that

- The source is a point source.
- The source and the receiver are located at the infinity from a lens object.
- The distribution of mass is spherically symmetric in an asymptotically flat spacetime (the lens object is a Schwarzschild black hole).

The bending angle of light α is

$$\alpha = \frac{4GM}{c^2 b} = \frac{2r_g}{b}, \quad (\text{B.1})$$

where G is the gravitational constant, M is the mass of lens object, b is the impact parameter of photon, c is the velocity of light, $r_g = \frac{2GM}{c^2}$ is Schwarzschild radius and we used weak field approximation ($\frac{M}{b} \ll 1$). This shows that the leading term of the bending angle of light is comparable to the first post-Newtonian effect.

Figure B.2 shows the geometry of a spherically symmetric gravitational lens by using the thin lens approximation where ξ is the impact parameter, D_S is a distance from the source S to the receiver R , D_L is a distance from the lens L to the receiver R , D_{LS} is a distance from the lens L to the source S , the source's true angular separation from the lens L is β , α is a bending angle by the lens L and the receiver sees an image of the source at angular position θ . The actual diameter can be described $[angle] \times [distance]$. However, this relation does not hold in curved spaces. Therefore, we can obtain the lens equation as

$$\theta D_S = \beta D_S + \alpha D_{LS}. \quad (\text{B.2})$$

By substituting Eq.(B.1) into Eq.(B.2), we obtain

$$\begin{aligned} \theta D_S &= \beta D_S + \frac{2r_g}{c^2 b} D_{LS}, \\ \theta D_S &= \beta D_S + \frac{2r_g}{c^2 \theta D_L} D_{LS}, \\ \theta &= \beta + \frac{\theta_E^2}{\theta}, \end{aligned} \quad (\text{B.3})$$

where we assume that $b = \xi$ and $\xi \approx \theta D_L$, θ_E is called the Einstein radius defined by $\theta_E^2 \equiv \frac{2r_g D_{LS}}{D_L D_S}$. Equation (B.3) determines the angle position θ of

the image as

$$\theta_{\pm} = \frac{\beta \pm \sqrt{\beta^2 + 4\theta_E^2}}{2}. \quad (\text{B.4})$$

In order to understand the Einstein radius θ_E , let us consider a case that the lens, the source and the receiver are aligned on a straight line. In other words, $\beta = 0$ case. In this case, the image becomes a circular ring called the Einstein ring. Then, the angle position of the Einstein ring is $\theta = \theta_E$. The Einstein radius θ_E is a characteristic angle for the gravitational lensing. In reality, the lens object is more complicated than the spherically symmetric lens. We measure the angle θ between the lens position and the image position from the observation, then we can determine the Einstein radius θ_E by using Eq.(B.3). If the distance from the receiver to the lens object and the distance from the receiver to the source can be obtained by another observation, the mass of the lens object is given by Eq.(B.2) and the definition of the Einstein radius θ_E . Therefore, the gravitational lensing can be used to measure the mass in the universe.

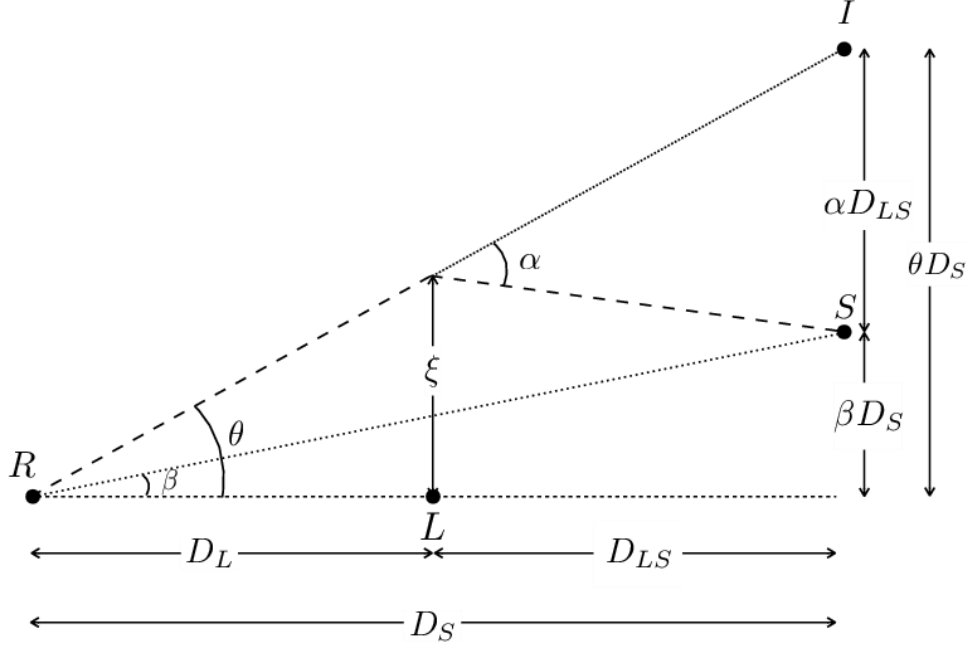


Figure B.2: Schematic figure for thin lens approximation. R is the receiver, L is the lens object at the distance D_L from the observer and S is the point source at the distance D_{LS} from the lens. We assume that $\xi = b$, then $\alpha = \frac{4GM}{c^2\xi}$. We presume that the angles (β, θ, α) are very small. β is the angular position of the source seen by the receiver. θ is the angular position of the image seen by the receiver.

Shear of image and magnification:

The changes in the shape and the brightness of finite size images are one of the important features of the gravitational lens effect. We assume that the separation angle of the finite size source is $\Delta\phi$. In the right hand side of Figure B.3, the two images are located at the angular positions θ_+ and θ_- given by Eq.(B.3). Due to the symmetry of the lens, the value ϕ of a light ray

is not changed by the gravitational lensing. In other words, the separation angles $\Delta\phi$ of the plus images is consistent with the separation angles of the minus images. By differentiating Eq.(B.4) with β , $\Delta\theta \equiv \frac{\partial\theta}{\partial\beta}$ is determined as

$$\Delta\theta_{\pm} = \frac{1}{2} \pm \frac{\beta}{2\sqrt{\beta^2 + 4\theta_E^2}}. \quad (\text{B.5})$$

Therefore, the image of a galaxy is sheared.

Gravitational lensing changes not only the shape of the image but also the brightness of the image. The change in brightness is used to find small mass objects.

The ratio of the brightness I_{\pm} of the image θ_{\pm} to the brightness I_* of the image without the gravitational lensing affected by the gravitational lensing can be expressed as the ratio of the solid angle $\Delta\Omega_*$ of the image without the gravitational lensing to the solid angle $\Delta\Omega_{\pm}$ of the image θ_{\pm} affected by the gravitational lensing. By using the relation for the solid angle in the polar coordinates $\Omega = \iint \sin\theta d\theta d\phi$, this ratio is

$$\frac{I_{\pm}}{I_*} = \frac{\Delta\Omega_{\pm}}{\Delta\Omega_*} = \left| \frac{\theta_{\pm}\Delta\theta_{\pm}\Delta\phi}{\beta\Delta\beta\Delta\phi} \right|. \quad (\text{B.6})$$

By using Eqs.(B.3) and (B.5), this equation becomes

$$\begin{aligned} \frac{I_{\pm}}{I_*} &= \left| \frac{\theta_{\pm}\Delta\theta_{\pm}}{\beta\Delta\beta} \right| \\ &= \frac{1}{4} \left[\frac{\beta}{\sqrt{\beta^2 + 4\theta_E^2}} + \frac{\sqrt{\beta^2 + 4\theta_E^2}}{\beta} \pm 2 \right], \end{aligned} \quad (\text{B.7})$$

where $\frac{I_{\pm}}{I_*}$ is called magnification. The magnification is always positive in this case, since $x + \frac{1}{x} \geq 2$ holds for arbitrary positive x . Therefore, the outer image of the Einstein ring becomes brighter ($\frac{I_{\pm}}{I_*} > 1$) and the inner image

gets darker ($\frac{I_{\pm}}{I_*} < 1$).

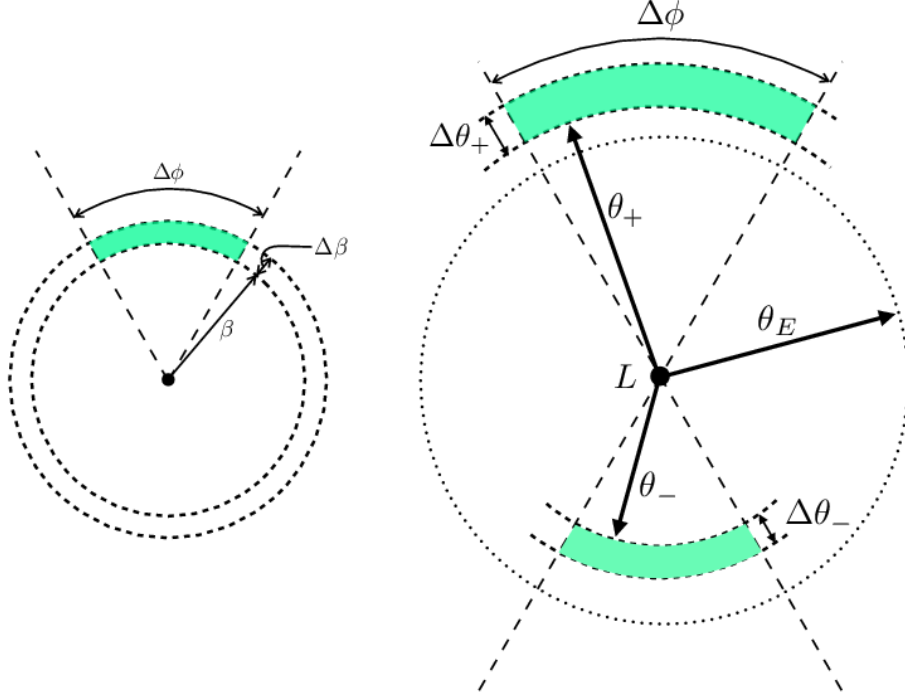


Figure B.3: Left: no gravitational lens. Right: the images sheared by gravitational lens.

Gravitational microlensing:

In the case of the microlens effect, the total magnification can be expressed from Eq.(B.7) as

$$\frac{I_{\text{total}}}{I_*} \equiv \frac{I_+ + I_-}{I_*} = \frac{1}{2} \left[\frac{\beta}{\sqrt{\beta^2 + 4\theta_E^2}} + \frac{\sqrt{\beta^2 + 4\theta_E^2}}{\beta} \right]. \quad (\text{B.8})$$

$\frac{I_{\text{total}}}{I_*}$ is always larger than 1. Therefore, gravitational lensing always cause a brighter image. This result is the reason that the gravitational lens effect

can be detected even though individual images cannot be decomposed.

It would be interesting to study an extension of the formulation of gravitational lensing, Eqs.(B.2) ~ (B.8) to a finite-distance situation.

References

- [1] L. D. Landau and E. M. Lifshitz, *The Classical Theory of Fields* (Pergamon, New York) 1962; S. Weinberg, *Gravitation and Cosmology* (Wiley, New York) 1972; R. M. Wald, *General Relativity* (The University of Chicago Press) 1984.
- [2] L. Blanchet, Living Rev. Relativ., **9** (2006) 4; S. Isoyama et al., Phys. Rev. Lett., **113** (2014) 161101.
- [3] M. A. Abramowicz et al., Astron. Astrophys., **521** (2010) A15.
- [4] V. P. Frolov and A. Zelnikov, Introduction to Black Hole Physics (Oxford University Press, Oxford) 2011.
- [5] L. Barack and N. Sago, Phys. Rev. Lett., **102**, (2009) 191101.
- [6] Z. Stuchlik and S. Hledik, Phys. Rev. D, **60** (1999) 044006.
- [7] A. Einstein, Ann. Phys. (Berlin) **49**, 769 (1916).
- [8] F. W. Dyson, A. S. Eddington, C. Davidson, Phil. Trans. R. Soc. A **220**, 291 (1920).
- [9] Y. Hagihara, Jpn. J Astron. Geophys. **8**, 67 (1931).
- [10] C. W. Misner, K. S. Thorne and J. A. Wheeler, *Gravitation*, (Freeman, New York, 1973).

- [11] C. Darwin, Proc. R. Soc. A **249**, 180 (1959).
- [12] V. Bozza, Phys. Rev. D **66**, 103001 (2002).
- [13] S. V. Iyer and A. O. Petters, Gen. Relativ. Gravit. **39**, 1563 (2007).
- [14] V. Bozza and G. Scarpetta, Phys. Rev. D **76**, 083008 (2007).
- [15] S. Frittelli, T. P. Kling, and E. T. Newman, Phys. Rev. D **61**, 064021 (2000).
- [16] K. S. Virbhadra and G. F. R. Ellis, Phys. Rev. D **62**, 084003 (2000).
- [17] K. S. Virbhadra, Phys. Rev. D **79**, 083004 (2009).
- [18] K. S. Virbhadra, D. Narasimha, and S. M. Chitre, Astron. Astrophys. **337**, 1 (1998).
- [19] K. S. Virbhadra and G. F. R. Ellis, Phys. Rev. D **65**, 103004 (2002).
- [20] K. S. Virbhadra and C. R. Keeton, Phys. Rev. D **77**, 124014 (2008).
- [21] S. Zschocke, Class. Quantum Grav. **28**, 125016 (2011).
- [22] E. F. Eiroa, G. E. Romero, and D. F. Torres, Phys. Rev. D **66**, 024010 (2002).
- [23] F. Abe, Astrophys. J. **725**, 787 (2010).
- [24] Y. Toki, T. Kitamura, H. Asada, and F. Abe, Astrophys. J. **740**, 121 (2011).
- [25] K. Nakajima and H. Asada, Phys. Rev. D **85**, 107501 (2012).
- [26] G. W. Gibbons and M. Vyska, Class. Quant. Grav. **29** 065016 (2012).
- [27] J. P. DeAndrea and K. M. Alexander, Phys. Rev. D **89**, 123012 (2014).

- [28] V. Perlick, Phys. Rev. D **69**, 064017 (2004).
- [29] T. Kitamura, K. Nakajima, and H. Asada, Phys. Rev. D **87**, 027501 (2013).
- [30] N. Tsukamoto and T. Harada, Phys. Rev. D **87**, 024024 (2013).
- [31] K. Izumi, C. Hagiwara, K. Nakajima, T. Kitamura, and H. Asada, Phys. Rev. D **88**, 024049 (2013).
- [32] T. Kitamura, K. Izumi, K. Nakajima, C. Hagiwara, and H. Asada, Phys. Rev. D **89**, 084020 (2014).
- [33] K. Nakajima, K. Izumi, and H. Asada, Phys. Rev. D **90**, 084026 (2014).
- [34] N. Tsukamoto, T. Kitamura, K. Nakajima, and H. Asada, Phys. Rev. D **90**, 064043 (2014).
- [35] G. W. Gibbons and M. C. Werner, Class. Quant. Grav. **25**, 235009 (2008).
- [36] M. C. Werner, Gen. Rel. Grav. **44**, 3047 (2012).
- [37] A. Ishihara, Y. Suzuki, T. Ono, T. Kitamura, and H. Asada, Phys. Rev. D **94**, 084015 (2016).
- [38] A. Ishihara, Y. Suzuki, T. Ono, and H. Asada, Phys. Rev. D **95**, 044017 (2017).
- [39] M. P. Do Carmo, *Differential Geometry of Curves and Surfaces*, pages 268-269, (Prentice-Hall, New Jersey, 1976).
- [40] T. Lewis, Proc. Roy. Soc. A, **136**, 176 (1932).
- [41] H. Levy and W. J. Robinson, Proc. Camb. Phil. Soc. **60**, 279 (1963).

- [42] A. Papapetrou, Ann. Inst. H. Poincaré A, **4**, 83 (1966).
- [43] In this thesis, we use the polar coordinates. The line element is known as the Weyl-Lewis-Papapetrou form in the cylindrical coordinates, [40–42].
- [44] H. Asada and M. Kasai, Prog. Theor. Phys. **104**, 95 (2000).
- [45] S. Kopeikin, and B. Mashhoon, Phys. Rev. D **65**, 064025 (2002).
- [46] V. Perlick, Phys. Rev. D **69**, 064017 (2004).
- [47] A. C. Belton, *Geometry of Curves and Surfaces*, page 38 (2015); www.maths.lancs.ac.uk/~belton/www/notes/geom_notes.pdf; J. Oprea, *Differential Geometry and Its Applications (2nd Edition)*, page 210, (Prentice Hall, New Jersey, 2003).
- [48] S. Chandrasekhar, *The Mathematical Theory of Black Holes*, (Oxford University Press, New York, 1998).
- [49] R. Epstein, and I. I. Shapiro, Phys. Rev. D **22**, 2947 (1980).
- [50] J. Ibanez, Astron. Astrophys. **124**, 175 (1983).
- [51] S. V. Iyer, and E. C. Hansen, Phys. Rev. D **80**, 124023 (2009).
- [52] F. P. Pijpers, Mon. Not. Roy. Astron. Soc. **297**, L76 (1998); S. L. Bi, T. D. Li, L. H. Li, and W. M. Yang, Astrophys. J. Lett. **731**, L42 (2011).
- [53] <http://sci.esa.int/gaia/>
- [54] <http://www.jasmine-galaxy.org/index-en.html>
- [55] E. Teo, Phys. Rev. D **58**, 024014 (1998).
- [56] Kimet Jusufi, and Ali Övgün, Phys. Rev. D **97**, 024042, (2018).

- [57] T. Ono, A. Ishihara, and H. Asada, Phys. Rev. D **96**, 104037 (2017).
- [58] P. Laguna and A. Wolszczan, Astrophys. J. **486**, L27 (1997).
- [59] L. Rezzolla and A. Zhidenko, Phys. Rev. D, **90** (2014) 084009.
- [60] K. Lake and T. Zannias, Phys. Rev. D, **92** (2015) 084003.
- [61] B. Carter, Phys. Rev., **174** (1968) 1559-1571.
- [62] S. Heisnam, International Journal of Astronomy and Astrophysics, **4**, 365-373.
- [63] A. Wünsch et al., Phys. Rev. D **87**, 024007 (2013)
- [64] T. Johannsen and D. Psaltis, Phys. Rev. D **83**, 124015 (2011).
- [65] P. D. Mannheim and D. Kazanas, Phys. Rev. D **44**, 417 (1991).
- [66] J. L. Said et al., Phys. Rev. D **88**, 087504 (2013).
- [67] G. V. Kraniotis, Class. Quant. Grav. **28**, 085021 (2011).